Selection of a DNA aptamer for the detection of human norovirus in meat

by

Amanda Giamberardino

BSc. (Hon), Carleton University, 2009

A thesis submitted to the Faculty of Graduate and Postdoctoral Affairs in partial fulfillment of the requirements for the degree of

Master of Science

in

Chemistry

Carleton University
Ottawa, Ontario

Your file Votre référence
ISBN: 978-0-494-83200-4
Our file Notre référence
ISBN: 978-0-494-83200-4

Abstract

In this study, DNA aptamer candidates for human norovirus were selected by an in vitro screening method called Systematic Evolution of Ligands by EXponential enrichment (SELEX). As human norovirus is considered a pathogenic organism, selection was performed on a commonly used norovirus model, murine norovirus (MNV). Following nine rounds of selection, the resulting pool was screened for sequences and was found to contain three potential candidates predicted to exhibit bulge and stem-loop structures. Preliminary binding studies by fluoresence anisotropy demonstrate a potential high-affinity candidate, with an estimated K_D of about 5.3 x 10^{-14} M for murine norovirus. The capsid of human norovirus strain, GII.3, was expressed and later used as a validation target with this candidate. Studies thus far suggest binding at close to the same magnitude. Both interactions appear to have a 5 to 6–fold higher affinity for norovirus over related virus feline calicivirus (FCV) and related tissue culture serums. Specificity was also demonstrated with a random nucleotide sequence alike in length, having an estimated binding constant of 10^{-7} M. The high-affinity candidate shows promise for later applications in an aptamer-based system to rapidly identify human noroviruses in meat products.

List of Abbreviations and Definitions

SELEX: Systematic Evolution of Ligands by Exponential Enrichment

BEVS: Bacculovirus Expression Vector System

VP1: major structural protein of norovirus (~60kDa).

VP2: minor structural protein of norovirus (~20kDa).

*Sf*9: insect cell line derived from *Spodoptera Frugiperda.*

TNM-FH/ Grace's media: Trichoplusia Ni Medium-Formulation Hinks; an insect media for *Sf*9 tissue culture.

Serum-free (insect) media: used for infections in BEVS.

MOI: multiplicity of infection.

pfu: plaque-forming unit.

VL-1, VL-3: baculovirus candidate samples for capsid genome for VP1.

AcNPV: *Autographa californica* nuclear polyhedrosis virus; wild-type bacculovirus acting as a positive control in BEVS.

XylE/XylE-pVL1392: Recombinant bacculovirus acting as a positive control in BEVS.

pVL1393: plasmid containing the GII.4 genome expressing the VP1 capsid.

GII.4: human Norovirus strain from Genogroup II, genotype 4.

GII.3: human Norovirus strain from Genogroup II, genotype 3

MNV: Murine (Mouse) Norovirus

FCV: Feline Calicivirus

FBS: Fetal Bovine Serum

LB: Lysogeny Broth; a bacterial medium

S.O.C.: Super Optimal Broth with Catabolite repression; a bacterial growth medium

pUC: control plasmid for cloning experiments.

X-Gal: 5-bromo-4-chloro-3-indolyl-β-d-galactopyranoside

DMEM: Dulbecco's Modified Eagle Medium

809: Stool sample containing GII.4 norovirus.

MB40: "Manitoba 40"; Stool sample containing GII.4 norovirus

W2: "Windsor 2"; Stool sample containing GII.4 norovirus

PAGE: polyacrylamide gel electrophoresis

SDS-PAGE: sodium dodecyl sulfate-polyacrylamide gel electrophoresis

Pool (5'→3') : CGT ACG GAA TTC GCT AGC -N_{40}- GGA TCC GAG CTC CAC GTG

Primer 1 (5'→3') : 6-FAM- CGT ACG GAA TTC GCT AGC

Primer 2 (5'→3') : A_{20}-HEGL-CAC GTG GAG CTC GGA TCC

Pr1u (5'→3') : CGT ACG GAA TTC GCT AGC

Pr2u (5'→3') : CAC GTG GAG CTC GGA TCC

6-FAM : 5'-Fluorescein Phosphoramidite, IUPAC: 6-(3',6'-dipivaloylfluoresceinyl-6-carboxamido)-hexyl-1-O-(2-cyanoethyl)-(N,N-diisopropyl)-phosphoramidite

HEGL: Hexaethylene glycol.

AG3 (5'→3') : 6-FAM-GCTAGCGAATTCCGTACGAAGGGCGAATTCCACATTG GGCTGCAGCCCGGGGGATCC

GSB: General Sensing Buffer.

List of Figures:

In Text:

In Appendix:

Table of Contents

I. Introduction

1. Food Safety and Foodborne Illness

Food safety plays a critical role in our everyday lives in ensuring the high quality and integrity of what we eat and drink. From farm to fork, safety measures are integrated throughout the food production chain to prevent contamination of food products and protect the public against foodborne illnesses. Figure 1 illustrates an overview of the food production chain [1]. The main steps of the chain are production, processing, distribution and preparation. Contamination of a food product can occur at any of these steps along the chain. In the production step, infected livestock, vegetation and water resources on farms, ranches and in the wild can provide a point of contact and introduce the contaminant into the process. Similarly, in processing, an infection can be introduced via contaminated materials. Unmaintained surfaces and cutting blades are one source of infection, which was thought to be responsible for the 2008 *Listeria monocytogenes* outbreak at a Maple Leaf Foods plant in Toronto [2]. Infection points may also occur through storage mediums (e.g. ice for packing or chilling produce) or pathogens that were previously present in an animal's intestines during the slaughter process. In the distribution step, the process in getting products from the farm or processing plant to the consumer or facility (restaurants, cafeterias, etc.) may be single or multi-staged. Contamination most often occurs in multi-staged distribution. Consider a scenario in which frozen hamburger patties might be transported from a meat processing plant to a large supplier, stored for a few days in the supplier's warehouse, transported again to a

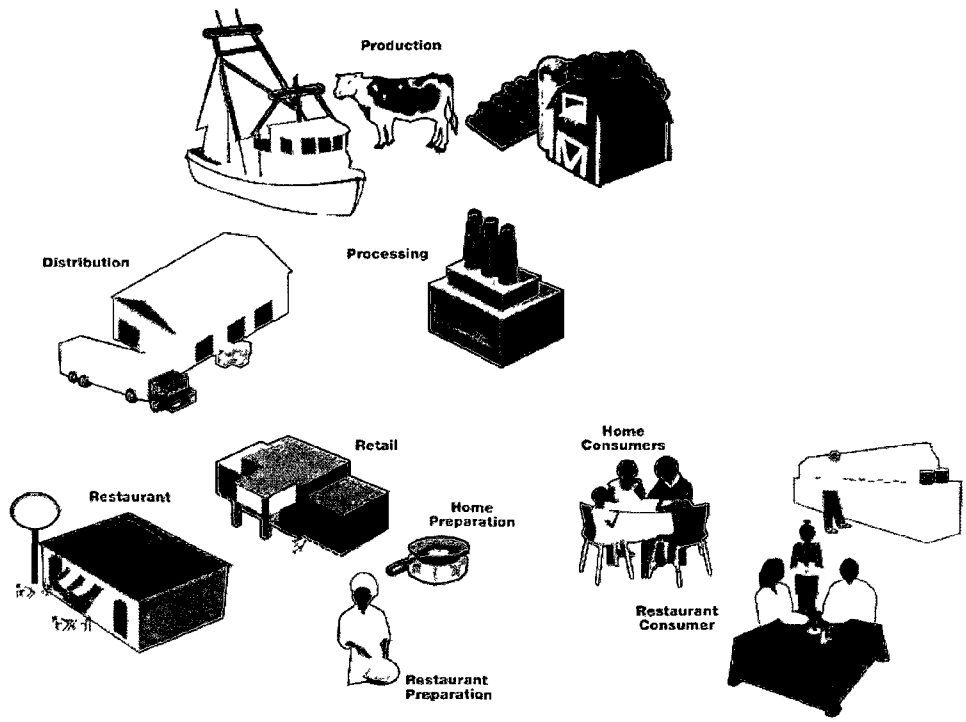

Figure 1-General schematic of the food production chain. [1]

local distribution facility for a restaurant chain, and finally delivered to an individual restaurant. If the food is subjected to any considerable period of time in warm temperatures or loaded onto a truck that was not cleaned from previously transporting other animal products, it provides a means for bacterial growth. In the preparation step of the food production chain, infection can occur in the kitchen of a restaurant, home or institute. It may involve following a complex recipe with many ingredients, simply heating and serving a food on a plate, or just opening a package and eating the food. The handler or materials used to prepare the food may already be infected and pass on the pathogen to the food. Moreover, the refrigeration of raw meat can introduce a contamination if its juice contacts other items that are eaten raw (e.g. vegetables).

Contamination may also occur through mishandling the food at multiple points. Once contamination occurs, further mishandling of food, such as undercooking the food or leaving it out on the counter at unsafe temperatures, can make an outbreak more likely. Many pathogens grow quickly in food held at room temperature where a tiny number can amplify to a large number in a few hours. Reheating or boiling food after it has been left at room temperature for a long time does not always make it safe because some pathogens (e.g. *Staphylococcus* enterotoxins, *Clostridium botulinum* spores) are not destroyed by high temperatures [3][4].

Although food safety regulations such as Good Agricultural Practice (GAP) and the Hazard Analysis Critical Control Points (HACCP) program [5] have already been established to prevent the most likely sources of contamination, the presence and persistence of pathogens in the environment make it challenging to control them totally, particularly at the farm level. Thus, the presence of pathogens in food should be anticipated and one should be able to determine which ones are present, in what quantities, and how the food can be protected or treated for optimum safety.

Foodborne pathogens are prevalent in Ontario accounting for about two-thirds of the incidences of gastroenteritis [6]; an inflammation or infection of the stomach and small intestine, constituting the gastrointestinal tract. It is sometimes referred to as a 'stomach bug', or, 'stomach flu' though it is not related to the Influenza virus. Major symptoms of gastroenteritis include diarrhea, nausea, vomiting and abdominal cramping. In some cases, fever and general weakness are additional symptoms. Gastroenteritis from food pathogens is not fatal and usually resolves itself within a few days (~48-72 hours).

However it does have a high occurrence and may trigger more serious complications in young infants, senior citizens and those with other underlying health conditions [7]. The most concerning complication is dehydration, since symptoms can upset the body's electrolyte balance and in extreme cases, may require intravenous administration of fluids to rehydrate the individual. Figure 2 lists some of the most common pathogens to trigger gastroenteric outbreaks in the United States, from 2007 to 2008 [8]. Although *E.coli O157, Campylobacter* and *Salmonella* are among the most predominant pathogens causing bacterial gastroenteritis, most outbreaks of gastroenteritis are caused by noroviruses.

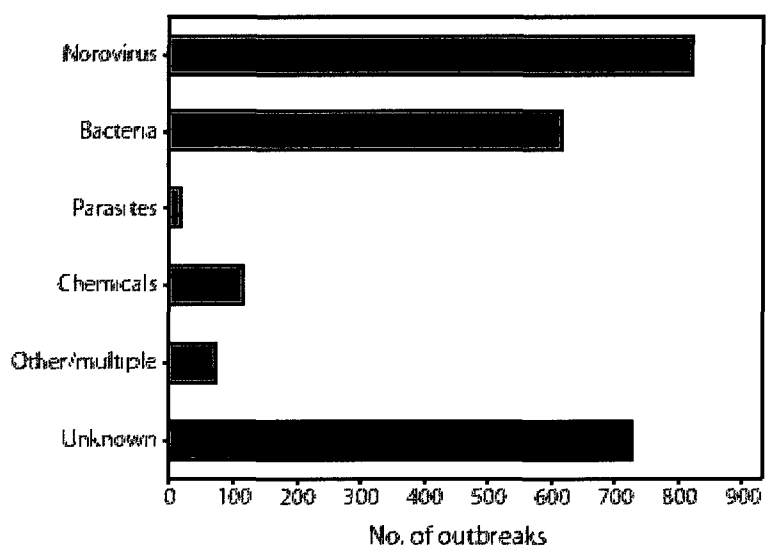

Figure 2-United States survey of foodborne disease outbreaks between 2007 and 2008. [8]

2. Noroviruses

Norovirus is responsible for more than 95% of acute non-bacterial gastroenteritis worldwide; with about 23 million reported cases per year in the United States alone [8,16]. It is sometimes referred to as "Norwalk Virus", named after the first identified case in 1972 at an elementary school in Norwalk, Ohio [9]. Contraction of this virus typically occurs through the fecal-oral route and via contaminated environmental surfaces. Foods passing through the food production chain can be exposed to the virus at various points, which include environmental introduction (e.g. contaminated water sources), food handling during processing and improper cooking of food. However with an infective dose as low as 10 viral particles [10], other routes of transmission (e.g person-to-person contact) are probable. Most studies of norovirus in food have historically focused on shellfish or imported fruits and vegetables but with respect to Ontario's food supply, the presence of noroviruses in meat products from cattle and swine also has relevance. Studies in cattle and swine feces have already demonstrated [11][12] that these viruses are able to survive processing and eventually end up contaminating uncooked meat products and ready-to-eat foods [13].

Norovirus-triggered gastroenteritis is typically characterized by symptoms such as a sudden onset of watery diarrhea, vomiting, abdominal pain, malaise, and a low-grade fever. Symptoms last anywhere between 1 and 3 days but virus shedding can continue anywhere from 2 weeks up to a year after overcoming symptoms [14]. In some cases, infected patients can be asymptomatic but still carry the virus, making it more

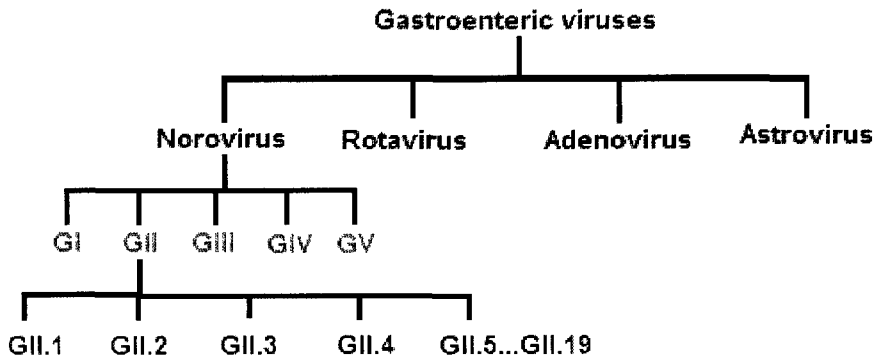

Figure 3- Classification tree of gastroenteric viruses with focus on the human Norovirus family. Genogroup nomenclature is defined by roman numerals whereas genotype nomenclature is organized by Arabic numbers.

challenging to monitor its transmission. People of all ages are susceptible to infection but more severe symptoms often occur in young children, the elderly and the immuno-compromised. Some evidence suggests an inherited predisposition to infection in individuals with O blood types [15] while the A, B and AB blood types can confer partial protection against symptomatic infection. The infection can occur throughout the year with a typical peak in the winter season.

Norovirus is a genetically diverse pathogen (Figure 3) having up to five different genogroups: GI, GII and GIV are human genogroups; GIII is a bovine genogroup and GV is a murine genogroup. Some strains from GII have also been isolated from swine and strains of GIV from feline and canine species [37-39]. Each of these is subdivided into many genotypes. For instance, the most prevalent human genogroup, GII, presently contains up to 19 different genotypes [8]. Current epidemic outbreaks of gastroenteritis in many countries have been linked to genotype four or more formally called the GII.4

strain. Since the mid-1990's, new variants of GII.4 have emerged every one to two years, which is typically followed by a cycle of increasing outbreaks [17]. Thus, there is a real risk of major norovirus epidemics.

Structural characteristics of norovirus virions include a single-stranded, positive-sense RNA genome that is 7.5kb in length and a subgenomic RNA sequence of 2.5kb. Both contain a poly(A) tail at the 3' end of their sequences. The RNA is linked with a small protein called VPg at the 5' end of the sequence, which has been found to play a key role in virus replication and RNA translation. Figure 4c illustrates three open reading frames (ORF) that describe the virus genome. ORF1 encodes for a polyprotein precursor which is cleaved by the viral protease into six non-structural proteins of an enzymatic nature. The genomic material is surrounded by a 30nm (diameter) capsid. The 58-60 kDa major structural capsid protein (VP1) is encoded by ORF2 and a 22-29 kDa minor structural protein (VP2) is encoded in ORF3, both of which are found in the genomic and subgenomic RNA. This conserved region is thought to play a role in initiating translation and also may facilitate the expression of structural proteins necessary for propagating virus assembly. It is still unclear as to the role of VP2 and while its function remains unknown, there is some evidence that VP2 may be involved in the stability of the capsid [18]. The capsid comprises of 180 copies (or alternatively, 90 dimers) of VP1 arranged in a three-fold icosahedral architecture [19] with one or two copies of VP2 within the capsid. Figure 4a shows a cryogenic electron microscope image of the capsids, which shares this general structure across the genus *Caliciviridae*. VP1 is comprised of various domains (Figure 4b): The N-terminus of the protein faces the interior of the capsid; the shell

domain (S-domain) which constitutes the continuous surface of the capsid; and the protruding domain (P-domain), which forms arch-shaped protrusion features and connects to the S-domain through a flexible short hinge. The P-domain is further divided into sub-domains (P1 and P2), corresponding to the leg and head of the protrusions and interact in dimeric contacts that increase the stability of the capsid. While P1 contains the C-terminus of the protein and is mostly conserved, P2 is the outermost surface of the capsid and contains the most variable sequences, which is considered key to understanding virus-host interactions and immune response [18].

2.1 Baculovirus Expression Vector System (BEVS)

Studies on human noroviruses are investigated through the VP1 capsid protein which can self-assemble into virus-like particles (VLPs). This is done using the Baculovirus Expression Vector System (BEVS), a popular method for producing recombinant proteins in eukaryotic cells. BEVS uses a helper-independent virus—the baculovirus, that can be propagated to high titres in insect cells making it possible to easily recover high amounts of recombinant protein. Its large viral genome can accommodate large segments of foreign DNA. Furthermore, the baculovirus promoters are inactive in mammalian cells which also allows for toxic proteins or oncogenes to be expressed and studied [21].

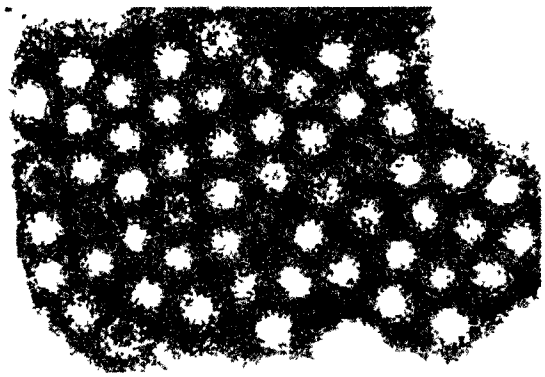

a

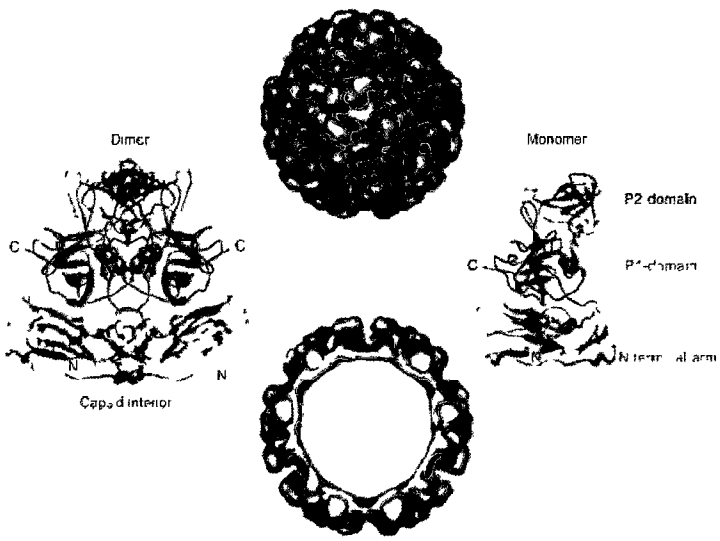
Dimer
Monomer
P2 domain
C
C
N
N
Capsid interior

b

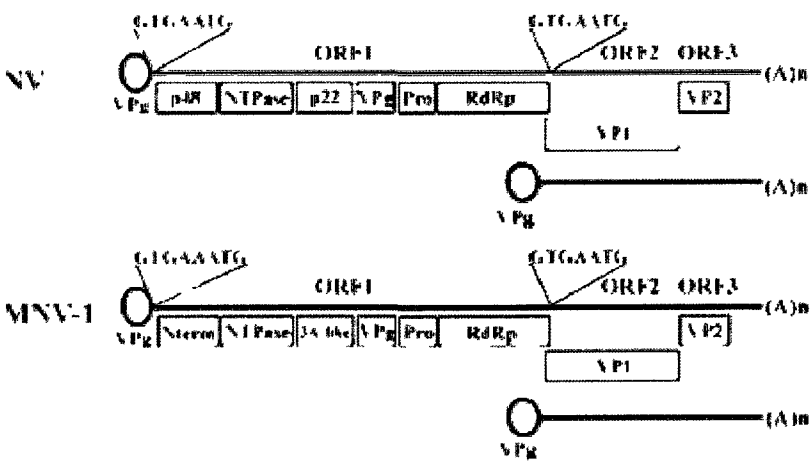
ORF1
ORF2
ORF3
(A)n
VPg
p48
NTPase
p22
VPg
Pro
RdRp
VP2
VP1
MNV-1
Pro
RdRp

c

Figure 4: Norovirus structural features. (A) electron microscope image of norovirus capsids [8]. (B) Structural features of the norovirus capsid. *top*: surface view; *bottom*: cross-sectional view; *left*: dimerized major structural protein, VP1; *right*: monomer major structural protein with labelled domains and subdomains [19] (Adapted with permission from Elsevier). (C) Genomic information of human norovirus (NV) and murine norovirus (MNV) [20] (Adapted with permission from the American Society for Microbiology).

The BEVS method can be described in the context of expressing the norovirus capsid. The VP1 gene is cloned into a transfer vector, which gets co-transfected with baculovirus DNA to form a recombinant baculovirus (Figure 5). The result is a genome that is infectious to two insect cell lines in *Spodoptera frugiperda* called *Sf* 9 and *Sf21* which are cells derived from larvae ovarian tissue [22]. Once a virus stock is obtained after co-transfection, recombinant virus is visually screened and purified using a plaque assay. The virus candidates are then amplified by re-inoculating cells at a low multiplicity of infection (MOI). The MOI is defined as the ratio of virus titer (in pfu/mL) to the number of cells inoculated. It comes from a statistical process that accounts for a percentage of cells that will absorb at least one viral particle. As MOI increases, so too does this percentage. For viral amplification, low MOI (< 1) is necessary to reduce the chances of introducing recombinant baculovirus with mutative genomes. Consequently, this is repeated a few times until a threshold titer is achieved to commence protein expression. The cells are then infected again (i.e. secondary infection) with this high titer stock at a high MOI (~3-10) to obtain optimal amounts of the secreted protein, as a result of the inserted gene.

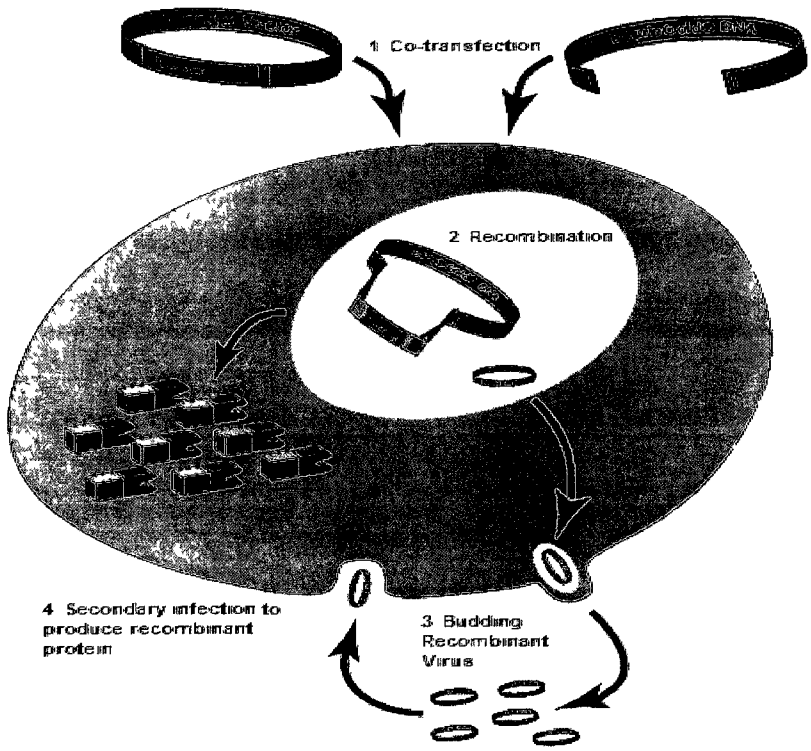

Figure 5: Schematic of Baculovirus Expression Vector System (BEVS). The gene of interest is inserted into a vector that recombines with baculovirus DNA (1) to form a recombinant baculovirus (2). This carrier virus infects *Sf*9 cells and is amplified (3) to produce a high titer stock which is eventually used in secondary infection of the cells (4) to produce recombinant protein as expressed by the inserted gene (Adapted from [22]).

2.2 Pathogenesis

Understanding norovirus pathogenesis remains challenging due to the lack of an effective cell culture system or animal model [21]. However, applications of recombinant VLPs have assisted in overcoming this challenge. For instance, VLPs have contributed in

determining the receptors involved in virus-host interactions. Human histo-blood group antigens (HGBAs) are receptors comprised of complex carbohydrates that exist on the surface of red blood cells and mucosal epithelia of the respiratory, genitourinary and digestive tracts [18]. They may also be present in saliva, intestinal contents, breast milk and the bloodstream. Based on various studies [15] [22], norovirus capsids have been shown to bind to HGBAs via a protein-carbohydrate interaction, which can be highly diverse and complex. As mentioned above, the P2 domain of the capsid is involved in binding to the host. It does so via the receptor (determined through various binding assays and crystallography studies) but occurs between two P monomer proteins, indicating the importance of the dimerization of the P domain. Hydrogen bonding is predicted to be the fundamental binding between fucose rings of the saccharide receptor and a GII.4 capsid (Figure 6) however, studies remain ongoing to better understand interactions with additional strains of the virus. With regards to norovirus entry and replication, various studies on the viral components have provided some progressing insight on their function and role in these processes [23]. For example, 3C-like protease ('Pro' in Figure 4c) was found to cleave Poly(A) binding protein in *in vitro* studies, which may inhibit cellular protein synthesis in infected cells. Another example is the RNA polymerase called 'RdRp', where upon interaction with recombinant VPg, produces a VPg-poly(U) component that may anneal to the poly(A) tail of the genome [24].

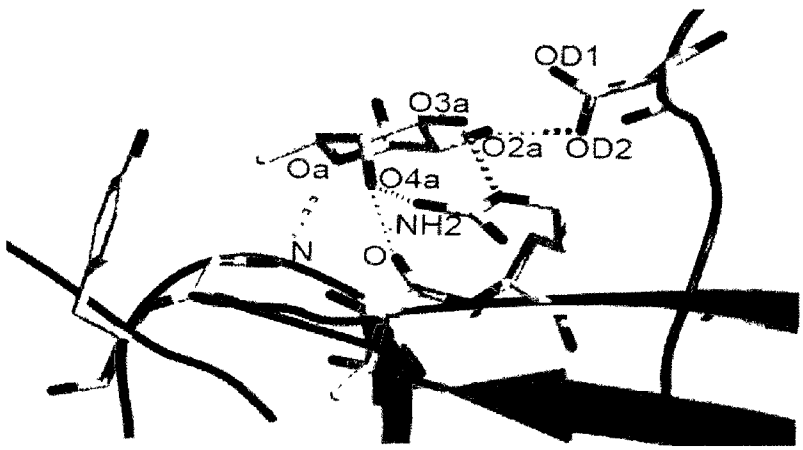

Figure 6: Receptor-binding interface of P-dimer (green and blue ribbons) of norovirus capsid and saccharide ligands (stick molecules) of HGBA receptor. Dotted lines represent hydrogen bonding from of nitrogen (purple), oxygen (red) and carbon (yellow) atoms. Other labels are assigned to various amino acid residues and atoms. (Adapted from[18]).

2.3- The MNV model

Norovirus is considered a class B biological agent [25] due to its high infectivity and stability and due to the suddenness of its outbreaks. Despite the significant economic impact and considerable morbidity caused by human noroviruses, no drug or vaccine is currently available to treat or prevent the disease. In addition, many aspects of norovirus biology are not yet fully understood. As previously mentioned, this is largely attributed to the absence of a cell culture system for human noroviruses. Murine norovirus (MNV) is the only norovirus that replicates in cell culture and in a small animal and is therefore the standard model for human norovirus studies to date [18]. MNV compares to human norovirus in a number of ways: i) it spreads via the fecal-oral route; ii) it has the same

diameter, shape, and buoyant density; and iii) it has three open reading frames (see Figure 4c). While ORF2 and ORF3 encode for the same structural proteins (M.W ~58.9 kDa and 22.1 kDa, respectively), ORF1 has some differences in its non-structural proteins. It has also been shown that the P domain of MNV is raised from the shell domain by about 1.6 nm and rotated by about 40 degrees clockwise. This results in new interactions at the P1 base that create a cage-like structure engulfing the S-domain [26]. Furthermore, upon BLAST sequence comparison between the two genomes, apparent differences in amino acid residues arise unsurprisingly in the P2 sub-domain. Unlike human norovirus VLPs, MNV is culturable with the RAW264.7 cell line [27] as well as mouse dendritic cells and macrophages. MNV asymptomatically infects wild-type mice and causes lethal neurological symptoms in STAT1 -deficient mice [28].

2.4-Diagnostic Methods of Norovirus

Currently, there are three diagnostic methods for noroviruses. The first method is visualization of the capsids under cryogenic electron microscopy as shown in Figure 4a. This is possible because their size is detectable on the nanometer scale and in fact, facilitated the discovery of the first noroviruses. However, this method is less sensitive since it requires a high viral load of approximately 10^6 particles per gram of stool sample [29]. With the development of Enzyme-Linked Immunosorbent Assay (ELISA) specifically for norovirus detection, smaller quantities could be identified. Expressed VLPs from BEVS behave as antigens in the assay and implements antibody reactivity as a means of detection. ELISA is useful because of its rapidity and simplicity for screening

many samples; however, because the capsids have variable regions, this can hamper specificity of the assay [18]. Additionally, there are the typical limitations that follow with antibodies: they are not always easily attainable, they can have batch-to-batch variation, they are costly, and they can have a short shelf life. The third and most widely-used diagnostic method is Reverse-Transcription Polymerase Chain Reaction (RT-PCR), which involves amplification of known, conserved regions of the norovirus genome using specific primers. The primer sets used so far have been developed for circulating strains as the genetic diversity of norovirus makes it impossible to use a universal primer set. Evidently, primer development is continuous for any newly discovered strains. Advancements in the RT-PCR method to improve sensitivity and fast detection include the use of real-time RT-PCR. This is the simultaneous amplification and quantification of the norovirus genome as it accumulates in real time. Different assay methods such as SYBR Green® and TaqMan® real-time PCR [30] have been developed to diagnose human and animal noroviruses. Particularly, the TaqMan probe in the latter methodology provides the advantage of confirming and quantifying results against a standard, in one assay. Among the three aforementioned diagnostic methods, real-time RT-PCR is the most sensitive [31-33], with a reliable detection limit of about 10 infectious particles [34]. Although it is considered the gold standard, a few challenges remain with this technique. First, one must account for PCR inhibitors that may be present in the sample (e.g. urea, excess salts, metal ions, and polysaccharides [35]) and will produce false negative results. Second, food samples, even when uncontaminated, are complex chemical matrices that may have other components obscuring data collection and analysis. This may require a sample preparation step, prior to the reaction to ensure optimum sensitivity and

specificity. Third, most real-time RT-PCR assays detect a highly conserved region of the norovirus genome but there can be slight differences in samples that can affect method performance. Therefore, one may not always distinguish between infectious and non-infectious norovirus in a positive PCR result. Finally, while non-perishable foods can be withheld until after results are available, perishable foods— particularly meat products and ready-to-eat foods, cannot be withheld due to their short turnaround time (about 8 hours). Thus, as a food safety technique, RT-PCR may not be able to consistently meet the pace of the meat production chain. To date, Krause *et al.* has demonstrated the detection of meat pathogens within this time period. However, the authors recommend that any rapid test method for the detection of pathogens in meat be portable and have a relative ease of use [36]. Therefore, an ideal norovirus detection system for use in the meat production chain should not only provide fast detection and be sensitive enough to detect the infectious dose or improve the LOD's of current methods, but also provide the additional benefit of portability and be easy to use.

3. Aptamers

Molecular recognition is the fundamental principle of biosensing and there is an increasing focus on developing new molecular recognition probes for food-safety related molecular targets. Antibodies have been considered the gold standard for molecular recognition elements and have been incorporated widely into biosensors and assays relating to food [40]. Despite their applicability to food monitoring, antibodies are not without their disadvantages. Antibodies are generated *in vivo*, which can be a costly process. Also, batch-to-batch reproducibility of antibody generation can be less than satisfactory. Compounding these limitations is their short shelf-lives and that they can be challenging to chemically modify precisely for incorporation into a biosensor platform. However, the affinity and specificity of antibodies for their molecular targets make them convenient receptors for biosensing strategies. Many of these disadvantages could be avoided with a molecular recognition probe of synthetic origin that could still maintain the required specificity and affinity. Because of their *in vitro* selection and production, the relatively new technology of aptamers [41][42] has emerged as a viable alternative for use in biosensor platforms.

Aptamers are described as short (~ 20-200nt) [43], single-stranded nucleic acids that can sometimes undergo a three-dimensional conformational change upon recognition of a target and do so with a comparably high degree of affinity and specificity. Targets, for which aptamers have been developed, range in size and nature from small molecules [44] to whole cells [45]. The *in vitro* nature of the selection process allows for the discovery

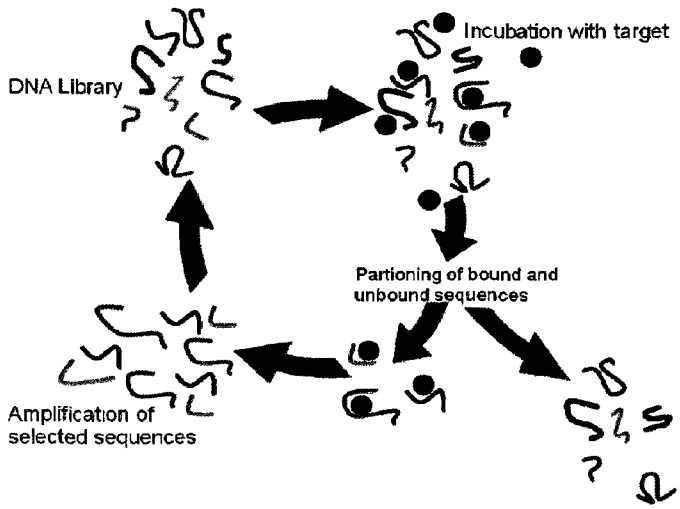

Figure 7: Schematic of the SELEX procedure for the selection of aptamer sequences. [47]

of aptamers for even non-immunogenic or highly toxic substances. In addition to this advantage, aptamers offer other benefits that are comparable to antibodies. First, high-purity aptamers can be chemically synthesized at a low cost and can be modified with dyes, labels, and surface attachment groups without loss or compromise of their affinities. Second, aptamers are more chemically stable under most environmental conditions, have a longer shelf life, and can be reversibly denatured without loss of specificity. These properties make aptamers attractive in the development of low-cost biosensors for diagnostic and therapeutic applications.

Aptamers are selected using an *in vitro* process called Systematic Evolution of Ligands by EXponential enrichment (SELEX), a procedure where target-binding oligonucleotides are selected from a random pool of sequences through iterative cycles of affinity, separation, and amplification (Figure 7). The SELEX process begins with a large

($\sim 10^{13}$ - 10^{15}), random oligonucleotide library whose complexity and diversity can be tailored through its distribution and number of random nucleotide regions [46]. These sequences are exposed to the molecule of interest and those with an affinity for the target are separated from non-interacting sequences. Elution of these binding sequences from the target and polymerase chain reaction (PCR) amplification of those binders yields an enriched pool for subsequent and more stringent selection rounds. This process repeats for several rounds after which the pool is cloned, sequenced, and characterized to obtain aptamers with the desired properties.

3.1 About SELEX

Although this describes the general process of SELEX, the technical steps are largely dependent on the nature of the target, the oligo library and the application of the desired aptamers. As a result there is no standardized protocol for an aptamer selection. There are five technical steps in the process of SELEX which will be herein discussed: i.) Binding, ii.) Partitioning, iii.) Elution, iv.) Amplification, and v.) Conditioning and vi) Cloning.

i. Binding

As mentioned above, aptamers may be selected for a wide variety of targets making SELEX technology in this sense a very flexible process. Evidently, not all targets will undergo an efficient selection. Aptamer selections can be more challenging if the target is

hydrophobic or a negatively charged compound. Target characteristics that support binding include intermolecular interactions such as positively charged groups (e.g. amino substituents), hydrogen bonds, and planarity (e.g. aromatics) [48]. Aptamer folding then permits for small molecule targets to be encapsulated by generating a binding pocket and for heavier targets like proteins to interact through the substructures at the surface of the target.

Nucleic acid libraries for the selection experiment typically contain a random core flanked by short, constant sequences for amplification. Certainly the random region can be designed in various ways. For example, one can have a completely random region which typically ranges from 20nt to 80nt [49]. In other cases where the random region is larger (> 90nt), it might be simpler to generate the pool in a modular manner by ligating shorter segments of oligonucleotides via restriction sites [50]. The former case is used to initiate SELEX when no functional nucleic acid sequence or structural motif is previously known. With regards to its complexity and length, it has been found that longer pools do not lose the numerical complexity of small pools and they gain access to some fraction of longer sequence and structural motifs. Although shorter-length pools offer more manageable and cost-effective syntheses, there is a loss of sequence space and therefore complexity is limited. Additionally, once aptamers are selected, sequences may be truncated to determine minimal aptamers—the smallest binding motif required to interact with the target. Another more novel way in which a random region may be designed is using segmentally random libraries which depend on experimental objectives such as improving the definition of a binding site by selecting wild-type mimics, or identifying a

binding site within the context of a known structural element [51]. The constant regions of the library, better known as "primer regions", are generally 20nt in length because their melting temperature makes them convenient for use in PCR and they can be easily synthesized in high yield. Primers must be designed so that they do not result in self-association and cross-hybridization, or, form secondary structures.

Another aspect for consideration is the type of aptamer to select: DNA versus RNA. In SELEX, RNA selections require a few extra transcription and reverse-transcription steps to preserve the RNA pool. To knowledge, there is no 'better' choice of aptamer; however, different schools of thought exist regarding their advantages and disadvantages. There are two main differences between DNA and RNA. The first is found in the pentose sugar of the oligonucleotide backbone. While RNA has hydroxyl (OH) substituents on the 2' and 3' position of the sugar, DNA lacks the OH substituent on the 2' position. This gives rise to the names "ribose" for the sugar units on RNA and "deoxyribose" for those on DNA. The second difference is that there is one different nucleotide of the four nucleotide bases. In DNA, the bases are adenine (A), guanine (G), cytosine (C) and thymine (T) however in RNA thymine is replaced by uracil (U) which differs from thymine with the absence of a methyl group. These structural differences between DNA and RNA cause these oligonucleotides to exhibit different chemical behaviours. Ribose is more reactive than deoxyribose because the C-OH bonds are susceptible to cleavage and thus are less stable than C-H bonds. DNA is also more stable in alkaline conditions than RNA since RNA can undergo hydrolysis of the phosphodiester backbone. Moreover, RNA is prone to ribonucleases found in most

biological materials. To overcome this, RNA can be modified with protecting groups (e.g. fluorine, hydrogen or an amino group) on the 2' position of the ribose or on the phosphodiester backbone [52]. Another way is to select a Spiegelmer [53]; an aptamer that binds to the enantiomer of the eventual target and is then synthesized as *its* enantiomer to be a nuclease-insensitive ligand of the normal target. In contrast, DNA is more susceptible to UV damage than RNA because the T bases can dimerize and form cross-linkages, upon prolonged exposure. Also, RNA has been reported to adopt a greater variety of secondary structures [54]. Nevertheless, the suitability of the aptamer type ultimately depends on its end application.

One considerably compulsory step in the SELEX experiment is to account for and reduce the possibility of non-specific interactions. This can be possible if the target is not completely purified for stability reasons; if there are unconcerned ions or molecules present; if the library can interact with the immobilization and/or partitioning medium; and if the target is combined with a structurally similar target (or "counter-target") in a real-world mixture. For these reasons, control selections in which the target is absent are incorporated before, during and after the selection. There are two main types of control selections: The first type is called a "negative selection" in which a library is partitioned in the absence of the target. The second type is called a "counter-selection" where the oligonucleotides are subjected to a similar target (i.e. a target with a slightly different structure) to improve aptamer specificity. In some cases, competitive selections are incorporated when the target has a high susceptibility to non-specific interactions to

nucleic acids and is done by simultaneous incubation of the target and library with other similar targets to obtain specific nucleic acid pools [55].

Selection stringency, which progressively increases from round to round, is another parameter to consider in a SELEX experiment. One simple way that this can be done is by changing the target concentration as the pool becomes more enriched. This creates a more competitive environment for the binding candidates to interact with the target of which only ones with the greatest affinity are retained. Other ways of introducing stringencies include modifications of binding and washing conditions including ionic strength, temperature, volume and reaction time of the sub-experiments.

ii. Partitioning

Partitioning is a critical step in the SELEX experiment since this is where binding sequences are separated from non-binding sequences. Target should be present in sufficient amounts and as pure as possible for optimal separation. For instance, it is impossible to conduct SELEX on a single molecule due to size restrictions. In these cases, aptamer partitioning on small molecule targets are typically done via affinity chromatography (i.e. solid supports such as columns or magnetic beads) in order to obtain binding sequences. In contrast, larger target molecules such as proteins and viruses can implement non-immobilization techniques including filtration or centrifugation [56]. This aspect of aptamer research is continuously growing, with more mechanical methods being developed and implemented. Instrumental methods such as capillary

electrophoresis [57] and Surface Plasmon Resonance [58] have been incorporated as partitioning strategies to efficiently isolate high-affinity aptamers for their targets. One study pioneered by Cox *et al.* has been working towards a completely automated SELEX experiment that could be completed in a few days, using an augmented pipetting instrument [59].

iii. Elution

Once the unbound molecules are discarded, the resulting target-nucleic acid complex is separated into its components, in order to isolate the binding sequences. Elution can be done using denaturing techniques (e.g. heat, urea, SDS, EDTA), affinity techniques (e.g. using the target) or using competitive binders [60].

iv. Amplification

The yield of binding sequences out of the initial 10^{15} sequences tends to decrease in a round of SELEX, since the nucleotide complexity of the pool is decreasing. Therefore, for ease of handling, amplification by PCR is often necessary to make more copies of the sequences of interest. At this stage, modifications (e.g. functional groups on primers) may be introduced for later detection and immobilization of the sequences. Moreover, this is where RNA and DNA diverge in terms of their amplification. While DNA can be directly amplified, RNA first needs to be reverse-transcribed into complementary DNA (cDNA) and then amplified. Asymmetric PCR may also be used to

favourably amplify the pool strand over the complement. There are unique methods that exist in which no amplification is required. One notable example comes from Berezovski and co-workers, termed as "Non-SELEX" [57], where they implemented non-equilibrium capillary electrophoresis of an equilibrium mixture to partition binding sequences from non-binding sequences. The process only involves two major steps: partitioning and analysis of the binding candidates. The low working volume for capillary electrophoresis makes this possible to perform.

v. Conditioning

Conditioning involves preparing the amplified pool for the next round of SELEX. DNA product from PCR is usually double-stranded as it comprises of the amplified pool sequence and its complement strand. Common methods to separate ssDNA product include the exploitation of the biotin-streptavidin interaction (e.g. on primer sequences for PCR, on magnetic beads), fluorescent labels or using size-exclusion methods. Williams and Bartel showed that double-stranded DNA could be easily separated by modifying one primer with a fluorophore and the other with a hexaethyleneglycol (HEGL) spacer and a poly (A) tail of 20nt (Figure 8). The spacer is a way to cease amplification by the DNA polymerase, '*Taq*'. Also attributed by the poly (A) tail, the size difference in the resulting strands becomes visible on a denaturing gel with UV or fluorescent shadowing [61]. This further allows for the pool to be monitored in later rounds.

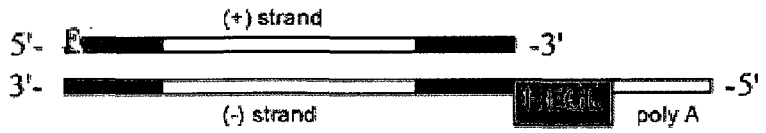

Figure 8: Amplification and/or conditioning of DNA using modified primers. The forward primer is fluorescently labelled to amplify the strand of interest (in this case the '+' strand). The reverse primer is modified with the HEGL spacer and poly(A) tail to add bulk to the amplifying complement strand (or '-' strand). This allows for better separation of single-stranded sequences on a gel [48] (Reproduced with permission from Elsevier).

vi. Cloning

Once the desired pool is selected, it is cloned to be later screened for the resulting sequences. The most convenient way to do this is by transformation in *E.coli* cells. This is because they are relatively simple organisms with a small genome; they replicate fairly quickly which cuts down experimental time and they readily take up foreign DNA (i.e. "competent"). It works by amplifying the pool by PCR with unmodified primers. The isolated product is then ligated into a vector that will be easily accepted by the host cell since the vector contains genetic information that is vital to the cell's survival. To assist the insertion of the vector, the cell-vector mixture undergoes a heat shock process by incubating them at relatively extreme temperatures and is spread on an antibiotic-treated culture plate. Upon incubation, the cells express visible isolated spots on the plate called colonies, which represent a single sequence from the pool. The colonies are then picked up and the foreign DNA is extracted and prepared for sequencing [63].

3.2 Binding studies

Once aptamers are selected, the next step to consider is sequence characterization. An aptamer's affinity for a target is generally defined by its dissociation constant (K_D), which will be discussed later in further detail (see Chapter 4). Binding constants for targets have been reported from micromolar scale (μM) [64] to as low as picomolar scale (pM) [65]. Although the choice of affinity experiment can depend on the target, most methods have great versatility and applicability. Such methods include affinity chromatography, affinity electrophoresis, equilibrium dialysis, filter binding assays, isothermal calorimetry, anisotropy and spectroscopic methods (e.g. UV-VIS, fluoresence, SPR) [66]. Notably, anisotropy will be further discussed in Chapter 4.

3.3 Applications of aptamers

With an ever increasing understanding of how aptamers interact with their targets, these nucleic acids demonstrate much potential in diagnostic and therapeutic applications [67, 68]. The challenge in creating such an "aptasensor" is to translate target binding into a measureable signal. In the context of food safety, there are already many aptamers that exist for food pathogens and toxins [69] but to date only a handful of those aptamers have reached the stage of sensor development. For example, Zelada-Guillén and co-workers reported the development of an electrochemical aptasensor using single-walled carbon nanotubes (SWNT) to selectively detect a non-pathogenic strain of *E.coli* cells called

CECT 675, serving as a model for the pathogenic strain O157:H7 [67]. Their motive for this aptasensor was to provide a simple, rapid and label-free means of detecting the target with comparably high sensitivity and selectivity. The sensor demonstrated robustness and stability in discriminating *E.coli* cells in spiked samples of apple juice and skim milk (Figure 9a) with LODs of 6 and 26 colony forming units per millilitre (*cfu*/mL). These detection limits are comparable with European regulated limits demonstrating the sensor's applicability in food testing. Incorporating O157 aptamers in a similar biosensor format therefore holds a great deal of potential. In another study, Bruno *et al.* developed a sandwich assay for the detection of *Campylobacter jejuni* [68]. The concept of the assay was based on aptamer-functionalized magnetic beads and CdSe/ZnS quantum dots. Two amino-functionalized aptamers are involved as the capture and reporter aptamers respectively attached to the magnetic beads and quantum dots. Equivalent amounts of the two aptamer-functionalized components were combined in a polystyrene cuvette to which *C.jejuni* bacteria was added. With the facilitation of a magnet, the probes are led towards one face of the cuvette and adhere to the surface. The reporter aptamer can then be measured by fluoresence in one plane with low background signal. Furthermore, the assay components can remain on the wall of the cuvette for weeks at ambient temperature. LOD of both the live and heat-killed bacteria were determined to be in the range of 10-250 *cfu/mL* in food matrices such as 2% milk, chicken juice and ground beef wash (Figure 9b). The authors further demonstrated that this detection system could be effectively used with a portable fluorometer, allowing for practical field-based detection. Cross-reactivity with other bacteria outside the *Campylobacter* family was very low but within the family was fairly high, indicating potential use for multi-strain detection.

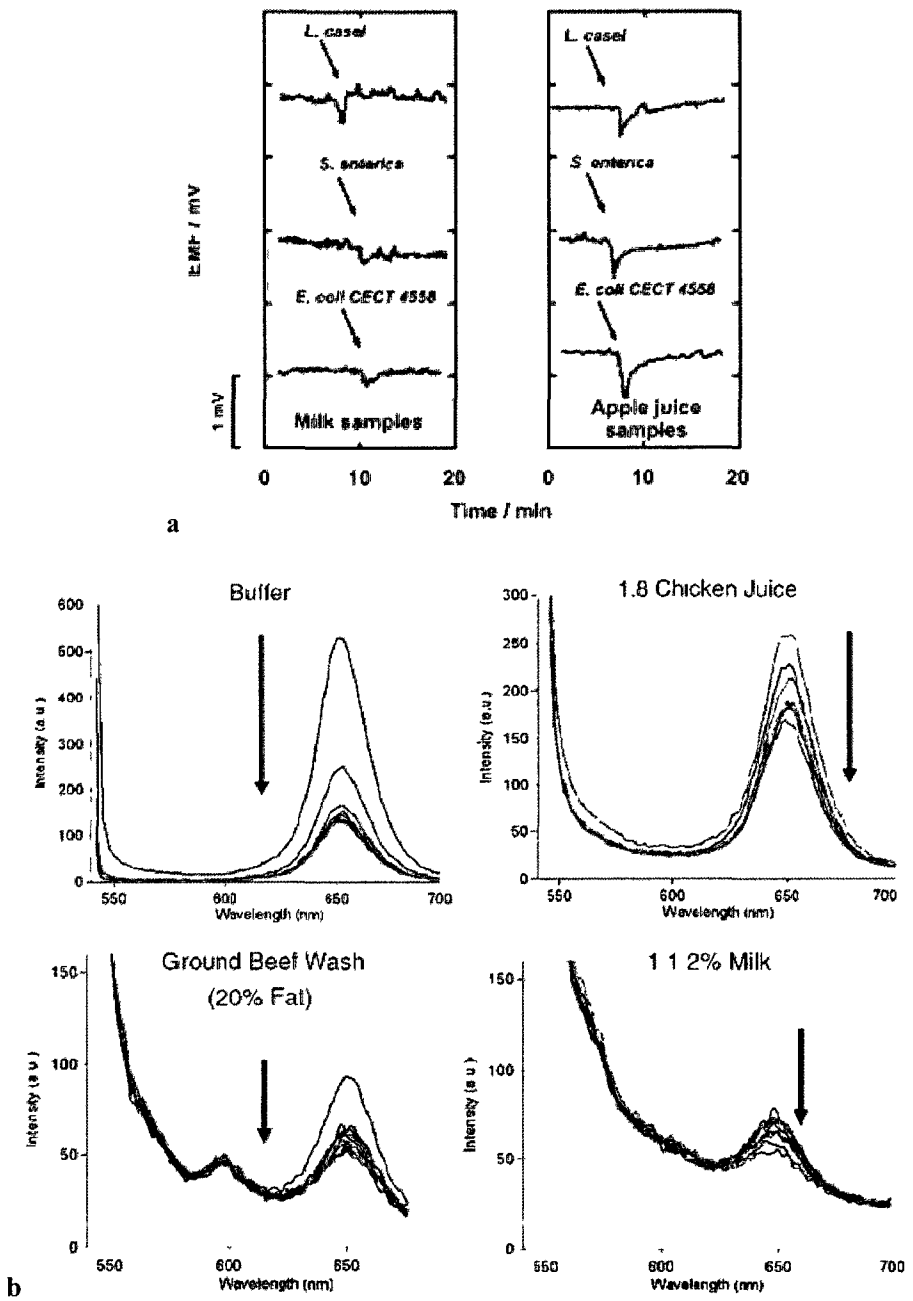

Figure 9: Examples of food safety aptasensors. a) Potentiometric response of SWNT-aptasensor specifically detecting *E.coli* CECT 675 cells in milk and apple juice matrices [67] (Reproduced with permission from the American Chemical Society). b.) Fluoresence emission spectra of *C. jejuni*

sandwich assay in buffer and three different food matrices. Arrows indicate decreasing amounts of bacteria measured [68] (Reproduced with permission from Springer).

Although these platforms are still in their infancy, they demonstrate much potential in future as practical food safety biosensors.

While the therapeutic potential of aptamers in food safety is still a relatively uncharted area of research, studies on other targets have been undertaken to exploit this characteristic. An FDA-approved aptamer commercially known as Macugen® binds to a vascular endothelial growth factor called VEGF 165 in the human eye in aim to prevent age-related macular degeneration. VEGF 165 promotes the formation of abnormal blood vessels eventually leading to blood leaks and eventual vision loss. Injection of the aptamer leads to binding with VEGF 165 and prevents the formation of these blood vessels by inhibiting the growth factor from binding to its receptor [70]. Another example is reported by Jang and co-workers who selected RNA aptamers to inhibit the coronavirus of severe acute respiratory syndrome (SARS). The aptamers were found to inhibit the double-stranded DNA unwinding activity of the virus' helicase component, demonstrating their applicability as antiviral agents [71]. Evidently, aptamers demonstrate much potential as practical tools for drug delivery and other therapeutic applications which could cross over into vaccinations against foodborne pathogens.

4. Characterization of Aptamer Binding

4.1 General principles

An important characteristic that defines an aptamer's affinity, or any receptor and ligand in general is the degree of binding with its target. This is usually defined by the dissociation constant, or "K_D" for short, which corresponds to the concentration at which 50% of the aptamer binds to its target, at equilibrium. In principle, the simplest case of a binding event would be one aptamer (A) binding to the target (T) to form a complex (C):

$$A + T \rightleftharpoons C \tag{1}$$

In which case, the K_D would be defined as

$$K_D = \frac{[A][T]}{[C]} \tag{2}$$

If one component (either [A] or [T]) is held constant while the other and [C] is measured, equation (2) takes the form of a titration curve that looks much like a strong acid-strong base titration curve (Figure 10). The midpoint of the linear spike in the curve represents the K_D. A lower K_D means more sensitive binding and thus higher affinity. This is the simplest case where the interaction stoichiometry is 1:1. Realistically however, in many biological systems and particularly in DNA-protein interactions, which are pertinent

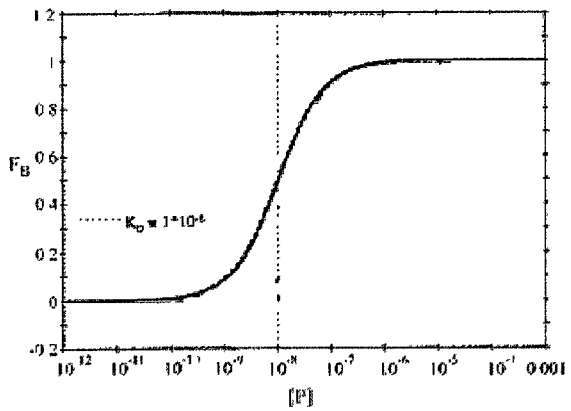

Figure 10: Example of an experimental equilibrium binding curve for an RNA aptamer (Adapted from [64]).

herein, more than one binding site may be involved and thus requires a modified model to further our insight into an aptamer-target interaction.[72]

4.2 The Hill equation

The common model that is used to describe interactions with proteins is called the Hill equation [73]. For an equilibrium interaction in which more than one binding site is involved, the reaction can be written as:

$$A + nT \rightleftharpoons AT_n \qquad (4)$$

Where 'n' is the number of binding sites. The apparent binding constant (K_n) can then be defined as:

$$K_n = \frac{[A]\times[T]^n}{[AT_n]} \tag{5}$$

With a multiple binding site target, it is important to differentiate between the macroscopic and microscopic binding constants. *Microscopic* would be with respect to a specific binding site whereas *macroscopic* would be with respect to the overall species. Usually it is the macroscopic binding constant that is assigned as the K_D and is what is easiest to measure experimentally as the microscopic constants would be difficult to distinguish.

Since the concentration of the complex $[AT_n]$ cannot be measured directly, we can infer it based on instrumental measurement and given the initial concentration of the aptamer and targets. This can be expressed as the fractional degree of saturation (ν_n) which is generally defined by:

$$\nu_n = \frac{n\times T^n}{K_n + T^n} \tag{6}$$

Cooperative binding is also a potential consideration in DNA-protein interactions. This happens when the interaction of one target and ligand facilitates the binding of another ligand. This phenomenon can be mathematically modelled by the Hill equation:

$$\nu_n = \frac{n\times T^{\alpha_H}}{K^{\alpha_H} + T^{\alpha_H}} \tag{7}$$

Where α_H is the Hill coefficient, a number that determines cooperativity and subject to the condition that $1 \leq \alpha_H \leq n$. So if $\alpha_H = 1$, there is no cooperativity but if $\alpha_H = n$, there is completely cooperative binding. If v_n is expressed as a function of known [T] or [A], the K_D can be derived by fitting the data to the function based on equation (7) where the value would be represented by the K^{α}_H term [74].

4.3 Fluoresence Anisotropy

Although there is a wealth of methods available to measure protein-DNA interactions, [65] in cases where there is a significant mass difference between the aptamer and its target, fluoresence anisotropy is one of the more common methods. Based on principles first described by Weigert F. Perrin [75], this technique measures an interaction between two species using plane-polarized light—that is, light in one direction is detected. Suppose the interaction is between a lightweight, fluorescently tagged ligand and a heavy receptor or target in a solution (e.g. a DNA strand and protein respectively). On its own, the tagged ligand is free to rotate in solution so when it is excited by plane-polarized light (Figure 11), it will scramble the polarization of light (or depolarize) by radiating its energy at a different direction from the incident light. However, upon binding with the heavy target, a larger and more stable complex is formed which will rotate or move in solution at a much slower pace. This reduces the "scrambling effect" on the emitted light so it remains mostly polarized and in the same plane as the incident polarized light.

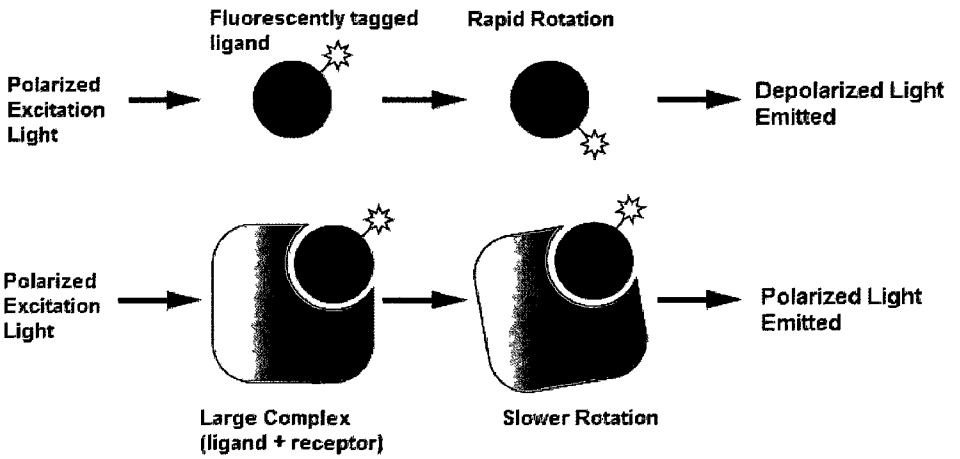

Figure 11: Schematic depicting the concept of fluoresence anisotropy. (Adapted from Invitrogen) [76]

Experimentally, the degree of this polarization is determined by measuring fluoresence intensity parallel ($I_{\|}$) and perpendicular ($I_{\perp}$) to the plane of polarized excitation light. It is expressed in terms of fluoresence polarization (P) but more conveniently expressed as anisotropy (r), which is proportional to the amount of ligand that binds. The values are mathematically related and interconvertable:

$$P = \frac{I_{\|} - I_{\perp}}{I_{\|} + I_{\perp}} \qquad r = \frac{2P}{(3-P)} \tag{8}$$

Polarization and anisotropy both represent a weighted average of the bound versus unbound states of the fluorescent species. Thus, by measuring the anisotropy at different target concentrations with constant ligand concentration, one can construct an equilibrium curve (as shown in Figure 10) where the midpoint in the curve represents the

K_D This technique works best if a small species is fused to a fluorophore and binds to a larger partner as this maximizes the difference in signal between bound state and unbound state. Conversely, if the fluorophore is attached to the larger partner in a binding event, the difference in polarization between bound state and unbound state will be smaller and less accurate to measure because the larger partner will already be fairly stable and inherently tumble slowly.

Aside from a measureable change between two interacting species, there are other advantages that make fluoresence anisotropy appealing. These include labelling with conventional and easily obtained organic dyes such as fluorescein and Texas Red, as opposed to using radioactive modifiers which are more expensive and also more hazardous to work with. It also eliminates the need for separation steps to purify complex from unbound ligands, thereby offering the opportunity to determine binding parameters such as the dissociation constant and also on/off rates by titration. Furthermore this makes it suitable for studies in high-throughput drug discovery and receptor research [76].

5. Project Objective(s)

The objectives of this study were to select a DNA aptamer for human norovirus and apply the aptamer in developing a field-based detection system for rapid identification of prevalent norovirus in contaminated meat samples. SELEX was to be used to select the aptamer against a norovirus model, MNV-1, while GII.3 and GII.4 norovirus capsid was cultured by BEVS for later binding and validation studies. The chosen SELEX method implements nitrocellulose filtration as a partition method to separate protein-DNA complex from free aptamer pool and also takes advantage of Flu-Mag SELEX techniques by using modified primers for pool amplification. Binding characterization was commenced by fluoresence anisotropy studies to assess a K_D for the interaction between ligand and target.

II. Materials and Methods

1. Preparation of Virus targets

1.1 List of Reagents

All reagents were used as received unless otherwise stated. Bacculogold Co-transfection kit, TOPO Cloning and QIAprep kits were previously purchased from Invitrogen and used according to the manufacturer's instructions.

1.1.1-Tissue culture media: a.) Modified Grace's medium (N.B. 50 mL of FBS and 10 mL of Streptomycin-Penicillin solution were added to Grace's insect media as supplements for cell growth) b.) Serum-free insect medium (both from Invitrogen)

1.1.2-1% Agarose solution (1% (w/v) SeaKem agarose in Grace's media + serum-free media)

1.1.3- SDS-PAGE reagents: a.) 30% acrylamide mixture (BioRad) b.) 1.5M Tris, pH~8.8 c.) 10% sodium dodecyl sulphate (SDS) solution d.) 10% (w/v) ammonium persulfate e.) TEMED f.) 1.0 M Tris, pH~6.8

1.1.4-17% sucrose in TEN buffer (100mM NaCl, 50mM Tris-HCl, pH 7.5; 1mM EDTA) [77]

1.1.5-General Sensing Buffer / SELEX buffer (50mM NaCl, 20mM Tris-HCl pH~7.4, 3mM $MgCl_2$, 5mM KCl)

All prepared buffers were filter-sterilized with Corning 0.45μm cellulose acetate filters before use.

1.2 Preparation of GII.4 norovirus capsid

All tissue culture procedures (with the exception of section 1.5) were carried out under a Labconco Biosafety cabinet.

1.2.1-Culturing Sf9 cells

A 1 mL vial of previously aliquoted *Sf* 9 cells was thawed from liquid N_2. Modified Grace's medium was thawed from 4°C storage to room temperature, using a water bath. About 15 mL of modified Grace's medium was pipetted into a cell culture flask (Corning® 175cm², angled neck with vent cap). The flask was stored in an incubator at 27°C until cells were equilibrated. The vial's contents were completely transferred by pipette and the flask was gently rocked back and forth to uniformly disperse the contents. The cells were left to attach for a minimum of 1h. The media was then removed and replaced with 20 mL of fresh modified Grace's media. The flask was incubated with media changes every 3-4 days until the cells became confluent. For splitting cells into additional flasks (e.g. 1 in 3), the media was replaced as

abovementioned followed by gentle tapping to detach the cells from the flask. To each of three flasks containing 15 mL of Grace's media, 5 mL of cell suspension was added and then incubated. (Note: Volumes of cell suspension added is dependent on the split pattern. A typical splitting process is 1 in 3 followed by 3 in 9, etc or until enough cells have been cultured for experimental use). For seeding cells, cell suspensions were transferred to a 50 mL Falcon tube and a 10µL aliquot was transferred to a hemocytometer. The hemocytometer was placed under a light microscope and cells were counted in each 4x4 quadrant. The cell density (cells/mL) was calculated to determine the equivalent volume required obtained the desired number of cells in a well/plate.

1.2.2-Preparation of pVL1393 plasmid for cloning

pVL1393 DNA stock was obtained from -20°C and thawed. Tubes containing 5 mL of LB media containing 20µL Ampicillin was obtained and thawed to 37°C. pVL1393 sample was stabbed with a pipette tip and the tip was dropped in the LB tubes. The tubes were incubated for 18 hours at 37°C. A miniprep of the plasmid was then conducted for purification, using a QIAprep kit as per the manufacturer's instructions and sent to GenScript® for insertion of the VP-1 genome (Minerva 2006b GII.4 norovirus, GenBank access #: EU078417) to create the recombinant vector (pVL+ GII.4).

1.2.3- Recombinant plasmid cloning of vector

Four reaction samples were prepared: Two experimental reactions with the received recombinant vectors ("pVL+ GII.4" and pUC+GII.4) and two controls (empty plasmid "pVL" and no plasmid). Four tubes of competent *E.coli* cells were thawed and placed on ice. Six LB-media plates were pre-warmed to 37°C using an incubator. To each tube of *E.coli* cells, 2μL of each sample was transferred and mixed gently by hand. The tubes were incubated on ice for about 5 minutes, heat shocked at 42°C for 30s and then immediately placed back on ice. To each tube, 250μL of S.O.C. medium was added. Tubes were capped, and shaked via shaker at 200rpm and 37°C for about 1h. LB-Ampicillin plates were prepared by adding 40 μL of X-Gal and 40μL of ampicillin to the prewarmed LB plates. Using a Lazy-L spreader, the X-Gal and ampicillin were evenly distributed across the LB plate in figure-8 motions. Each plate was labelled and inoculated with a reaction tube as follows: *1*-10 μL of "pUC+GII.4"; *2*-50μL of "pUC+GII.4"; *3*-10μL of "pVL+ GII.4"; *4*-50μL of "pVL+ GII.4"; *5*- 50μL of "pVL" (empty plasmid); *6*-negative control (cells + 50μL of H_2O). Plates were incubated at 37°C overnight and ten colonies (5 "pUC+GII.4" and 5 "pVL+ GII.4") were picked using blue-white screening. The colonies were stabbed with pipette tips and suspended in tubes containing 5 mL of LB media and 20μL ampicillin. Tubes were incubated for 18 hours at 37°C. 1.5 mL of each inoculated culture was transferred to microcentrifuge tubes. Miniprep was conducted as previously described (section 1.2.2).

1.2.4-Agarose Gel Electrophoresis for visual characterization of plasmids.

A 1% agarose gel mixture was prepared by weighing ~1.0g of electrophoresis grade agarose (Sigma) combined with 100 mL of 0.5X TBE buffer. The solution was microwaved for about one minute or until the agarose completely dissolved. The suspension was allowed to cool to touch and 2µL of SYBRSafe dye was added and mixed. The mixture was gently poured into a tray with a small-tooth comb and allowed to polymerize for at least 15 minutes. The comb was then removed and the tray was placed in the electrophoresis unit (Mandel Scientific) and covered with 0.5X TBE as the running buffer. Samples were prepared as follows: For each 2µL sample, 2µL of Nucleic Acid loading buffer (BioRad) was added (note: maximum load of a well was 5µL). An additional sample comprised of 2µL DNA LADDER (1kb, BioRad) and 2µL of Nucleic Acid loading buffer was prepared. Each sample was loaded into the agarose gel. The gel ran for 30 minutes at 135V and was visualized using a FluoroImager under the 'Ethidium Bromide/Syber Green' channel. (see figure A1 in Appendix)

1.2.5-Co-transfection of Sf9 cells

Co-transfection was performed with a Bacculogold co-transfection kit (Invitrogen) [22]. Briefly, 2 x 10^6 *Sf 9* cells were seeded per well (see section 1.2.1) in a 6-well plate (Corning 3516, Costar) and allowed to attach for 1h. Meanwhile, co-transfection samples were prepared as follows: Experimental samples consisted of 5µL of linearized Bacculogold DNA and 1µL of the plasmids (pVL+ GII.4) in a microcentrifuge

tube. These were mixed by gentle vortexing and allowed to stand for 5 minutes after which 1 mL of Transfection Buffer B was added. Similarly, a positive control sample containing AcNPV was prepared with 5μL of linearized Bacculogold DNA and 20μL of AcNPV vector followed by 1 mL of Transfection Buffer B. The media from the plates was aspirated and replaced with 2-3 millilitres of serum-free insect media plus 1 mL of Transfection Buffer A. Wells were inoculated with 1 mL of co-transfection sample dropwise about the well circumference and then rocked gently to mix thoroughly. Plates were incubated at 27°C for ~4hrs. Media was removed (and transferred to 15 mL falcon tubes for storage) and replaced with 3 mL of serum-free media. Plates were incubated at 27°C for 4-5 days and checked for signs of infection.

1.2.6-Plaque assay for viral purification

Cells were seeded 4.2 x 10^6 per well (see section 1.2.1) onto 60mm tissue culture plates (Costar) (20 plates for experimental samples and positive control, 1 plate for negative control) and allowed to attach for ~1h. Serum-free media was removed and replaced. To each plate, 100μL of serially diluted virus inoculum (10^0-10^{-2} of pVL and AcNPV in duplicate) was added dropwise about the circumference of the plate. Plates were incubated for at least one hour at 27°C. A 1% (w/v) SeaKem agarose solution in serum-free media was prepared and heated in 30s intervals in a conventional microwave until agarose dissolved (about 1.5 minutes in total). The solution was kept warm at 50°C in a water bath until ready to use. The media from the plates was then removed and overlaid with 6 mL of the 1% agarose solution. The plates were allowed to stand for

about 20 minutes at room temperature to solidify the developing agarose plugs. Plates were incubated at 27°C for 6-10 days and checked for plaque formation under a light microscope. Ten plaque-containing plugs were identified and picked up using autoclaved micropipette tips and transferred to microcentrifuge tubes containing 1 mL of serum-free media. The virus particles were eluted out of the agarose plug by rotating the tubes overnight at 4°C in an incubator. Following incubation, 200µL of each plaque pickup was added to a separate well of a 12-well plate (Cat#9202, TRP) seeded with 2 x 10^5 cells in 1 mL of fresh serum-free media. Plates were incubated at 27°C for 3 days. The viral supernatant of this passage one (P.1) stock was collected and centrifuged for 5 minutes at 1000g at 4°C using a Rotanta 460R centrifuge to remove cell debris. For each stock, a 6-well plate was seeded with 1.8 x 10^6 cells per well as previously described (section 1.2.1). P.1 virus stocks were added to each plate and incubated at 27°C for 3 days (to become P.2 virus stock).

1.2.7-Plaque assay for viral quantification (titer assessment)

Six-well plates were seeded with ~1.8 x 10^6 cells per well and diluted in serum-free media. The cells were allowed to attach for ~1hr after which serum-free media was changed. The cells were inoculated with 100µL of serially diluted P.2 virus stocks (10^0-10^{-4} or lower depending on titer stocks) in duplicate and left to be infected for about 1.5hrs. The suspension media was removed and the wells were overlaid with 5 mL of 1% SeaKem agarose solution (see section 1.2.6). The plates were left to stand for 20 minutes to allow the agarose solution to solidify. The plates were then incubated at 27°C for 6-10

days after which plaques were counted to assess viral titer (*pfu*/mL). For further enhancement of plaque visualization, agarose plugs were removed by treatment with 1 mL of 4% para-formaldehyde (PFA) for 4h. The PFA was then drained and plugs were dislodged by gently applying pressure with water. To each well, 1.5 mL of 0.1% crystal violet staining solution was added. Plates were incubated for 20 minutes after which wells were drained.

1.2.8-Amplification of GII.4 bacculovirus

100mm plates were seeded with 1.0 x10^7 cells each and diluted with 10 mL of serum-free media. Plates were allowed to attach for 1hr. Media was replaced and the cells were infected at a low multiplicity of infection (MOI~0.1) using 1 mL of P.2 virus stock. Plates were incubated for about 7 days, while monitoring progress of the infection (see figure 13). Viral supernatant was harvested and titer was assessed by plaque assay as previously described (section 1.2.7). Amplification and plaque assay procedures were repeated until a minimal titer (usually ~1 x 10^8 *pfu*/mL) was achieved for protein expression.

1.2.9-Protein Expression of GII.4 capsid.

Plates were seeded with ~1.2 x 10^6 cells per well. Media was replaced and plates were inoculated with virus at a high MOI (MOI~3; corresponded to an inoculation volume of ~3.6 mL). Plates were incubated at 27°C for 3 days (see figure 15 for

observations) after which the supernatant containing secreted protein was harvested. Samples were centrifuged at 10,000g for 5 minutes, using a Spectrafuge benchtop centrifuge to remove pelleted cell debris and stored at 4°C until needed. Characterization was conducted by SDS-PAGE (described below in section 1.3.4).

1.3 Preparation of GII.3 norovirus capsid

1.3.1- Amplification of GII.3 baculovirus

GII.3 virus stock was used (as received) (titer~10^7pfu/mL) to infect 1.33 x 10^7 *Sf*9 cells at a low MOI of 0.25 (corresponds to an inoculation volume of about 400µL), on a 100mm tissue culture plate. Negative and positive (XylE-pVL1392) controls were simultaneously prepared for comparison. The plates were incubated at room temperature (27°C) for 5 days, after which the supernatant was harvested to remove from cell debris. This was done at 10,000g for 5 minutes at room temperature using a benchtop centrifuge.

1.3.2- Plaque Assay on Amplified GII.3 baculovirus

6-well plates were seeded with 1 x 10^6 cells per well diluted in serum-free media. The cells were allowed to attach for ~1hr, after which serum-free media was changed. Cells were then inoculated with serial dilutions of the amplified virus (10^0-10^{-10}) in duplicate and left to be infected for about 1.5hrs. The suspension media was removed and

the wells were overlaid with 5 mL of 1% agarose solution (pre-warmed to 45°C). The plates were left to stand for 20 minutes to allow the agarose solution to solidify. Plates were then incubated at 27°C for 6-10 days after which plaques were counted to assess viral titer (*pfu*/mL).

1.3.3-Protein Expression of GII.3 VP1 capsid

Protein expression of the GII.3 capsid was conducted at three different MOI (4, 6 and 8) by inoculating with respective volumes of virus stock (titer~2 x 10^8 pfu/mL; these were 275µL, 410µL and 540µL, respectively) on 1.33 x 10^7 cells seeded on 100mm plates. The plates were incubated for 3 days at 27°C and the virus was harvested to isolate it from cell debris (10,000g, 5 minutes).

1.3.4. SDS-PAGE characterization of capsids

Note: All buffers and virus stocks in this procedure were used as received unless otherwise stated.

The following ingredients were combined for casting a 12% polyacrylamide resolving gel [78] in duplicate: 6.6 mL distilled H_2O, 8.0 mL 30% acrylamide mix, 5.0 mL 1.5M Tris buffer (pH ~8.8), 0.2 mL 10% SDS, 0.2 mL 10% ammonium persulfate

and lastly 8μL Tetramethylenediamine (TEMED). The mixture was poured between preassembled glass plates and 2 mL of isopropanol was immediately overlaid. The gel was allowed to polymerize for 30 minutes. Meanwhile, the following ingredients were combined for casting a 5% polyacrylamide stacking gel: 5.5 mL distilled H_2O, 1.3 mL 30% acrylamide mix, 1.0 mL 1.0M Tris buffer (pH ~6.8), 0.08 mL 10% SDS, 0.08 mL 10% ammonium persulfate and lastly 8μL TEMED once ready to pour the gel. The isopropanol was drained out, the stacking gel was loaded and the combs were set in the stacking gel. The gel was allowed to polymerize for 30 minutes. Samples were prepared by adding 1 equivalent of Laemmli buffer (BioRad) and placed on ice until needed. Gel-casted plates were assembled in the electrophoresis unit (MGV-202, C.B.S & Scientific Co.) filled with 1X running buffer (diluted from a 1L-10X stock containing 0.25M Tris base, 2M Glycine and 0.03M SDS). The gel was pre-equilibrated at 120V for 10 minutes. Prior to loading, samples were heated at 95°C for 5 minutes and then placed immediately on ice. A sample containing 1kb Protein LADDER (Precision Pro Dual Colour, BioRad) was heated for one minute and then placed on ice. Samples were loaded (maximum of 20μL) on the gel and ran at 120V for about 1.5hrs or until the dye front reached the bottom of the gel.

The gel was suspended in Coomassie Blue stain for about 20 minutes and then suspended in destaining solution (30% (v/v) acetic acid, 10% (v/v) methanol) overnight to remove excess Coomassie Blue and for optimal band visualization. Imaging was done with an Alpha Innotech FluorImager under the 'white transluminesence' channel.

1.3.6 Purification of GII.3 capsid

Purification by sucrose was adapted from [77]. Briefly, the sample was centrifuged at 12,000rpm for 20 minutes to separate cell debris. The supernatant was removed and divided between 38.5 mL Beckman UltraClear^{TM} centrifuge tubes atop a layer of 36 mL of 17% sucrose in TEN buffer (see section 1.1). The samples were centrifuged using a Beckman-Coulter Optima L-90K ultracentrifuge at 27,000 rpm for 3 hours to force the heavier capsids to the bottom of the tube. Supernatant was removed and the sample was re-suspended in GSB buffer (section 1.1) for dialysis purification (see section 1.4)

1.4 Purification and characterization of virus stocks (MNV, GII.3, FCV, DMEM and Grace's Media)

Prior to aptamer selection, all virus stocks were dialyzed into SELEX buffer (GSB buffer--see section 1.1) acting as the exchange buffer. Clipped snakeskin tubing and Slide-A-Lyzer cassettes (ThermoFisher Scientific) were prepared according to the manufacturer's instructions. The tubing and cassettes, containing the volume of virus, were incubated in 200x volume of stirred exchange buffer for a minimum of one hour at room temperature. Buffer was changed and the suspension was allowed to incubate with continuous stirring overnight at room temperature. The equilibrated samples were then

concentrated down using Amicon Ultracell 50K (50,000 MWCO) filter tubes according to the manufacturer's instructions.

Samples were characterized by either UV-Vis absorption using a Cary Bio300 spectrophotometer with a Starna 50uL quartz cell or a ThermoScientific NanoDrop 1000 wherever possible. Absorbance was measured at λ=280nm. Extinction coefficients as follows: ε_{MNV} =72,560 $M^{-1}cm$; $\varepsilon_{GII\,3}$ = 47,058 $M^{-1}cm$; ε_{FCV} =105,000 $M^{-1}cm$ [79]

2. Aptamer selection on murine norovirus (MNV)

2.1 List of Reagents

All amidites for DNA synthesis were purchased from Glen Research. All standard chemical reagents were purchased from Sigma unless otherwise stated. Deionized water obtained through a Milli-Q water filtration system (Millipore) was used for all experiments. PCR reagents (Taq Polymerase, 25mM $MgCl_2$, 10mM dNTP), were purchased from BioShop. PCR tubes (0.2 mL) and microcentrifuge tubes were purchased from Diamed. Gel electrophoresis ingredients were purchased from BioShop.

2.1.1- DNA suspension buffer (10mM Tris-HCl, pH~7.4)

2.1.2- General Sensing Buffer / SELEX buffer (50mM NaCl, 20mM Tris-HCl pH~7.4, 3mM $MgCl_2$, 5mM KCl). See also section 1.1.

2.1.3- Elution buffer (7M urea, 50mM HEPES-NaOH, pH~7.5, 10mM EDTA) [80]

2.1.4- 3M NaCl

2.1.5- Flu-Mag PCR buffer (100mM KCl, 200mM Tris, 2% Triton X-100, pH~9)

2.1.6- 5X TBE buffer for denaturing PAGE (0.445M Tris, 0.445M Boric Acid, 0.010M EDTA, pH~8.3)

All buffers were filter-sterilized with Corning 0.45μm cellulose acetate filters before use.

2.2 DNA Synthesis (pool, PCR primers, AG3)

All sequences (pool, modified and unmodified primers [81] and aptamer candidates) were synthesized on a MerMade 6 automated DNA synthesizer using 500Å controlled pore glass (CPG) columns. Nucleotide sequences defined as follows (5'→3'). ***Pool sequence***: CGT ACG GAA TTC GCT AGC- N_{40} -GGA TCC GAG CTC CAC GTG; ***Primer 1***: (6-FAM)-CGT ACG GAA TTC GCT AGC; ***Primer 2***: A_{20}-HEGL-GTG GAG CTCGGATCC-3; ***AG3***: (6-FAM)-GCT AGC GAA TTC CGT ACG AAG GGC GAA TTC CAC ATT GGG CTG CAG CCC GGG GGA TCC; ***AG28***: (6-FAM)- CGT ACG GAA TTC GCT AGC ACG GGG CTT AAG GAA TAC AGA TGT ACT ACC GAG CTC ATG AGG ATC CGA GCT CCA CGTG; ***AG29***: (6-FAM)- CGT ACG GAA

TTC GCT AGC CGA CGG TCA ATG CTC GTG AGC CAG TAC ACA CAA TAT ATG TGG ATC CGA GCT CCA CGTG; N.B. Unmodified primers (Pr1u and Pr2u) have the same nucleotide sequence as Primers 1 and 2 except without fluorescein or polyA-HEGL modifications (see also List of Abbreviations and Definitions). Preparations of the sequences are as follows: Immobilized DNA on the CPG beads of the column was deprotected for 16h with 1 mL of 28% NH_4OH at 55°C. The CPG beads were separated from NH_4OH-DNA using filter tubes (Spin-X 0.22μm cellulose acetate, Costar) and centrifuged at 4,000 *g* for 5 minutes. NH_4OH was evaporated from the DNA with a Savant AES2010-220 speedvac concentrator. The DNA was re-suspended in 10mM Tris buffer, pH~7.4 and isolated from failed sequences by denaturing PAGE (section 2.4). Bands were excised from the gel and suspended in 6 equivalents volume of 10mM Tris buffer, pH~ 7.4. The DNA was eluted by heat shock at 50°C for five minutes, 90°C for 5 minutes and overnight rotation at 37°C in a bench-top incubator (ThermoFisher Scientific). Gel was filtered from DNA suspension with 0.45μm syringe filters (Pall) and lyophilized to working volume using a Labconco FreezeZone 4.5 freeze dryer. DNA was then purified by ethanol precipitation: mixed with 0.5 x volumes of 3M NaCl and 10 x volumes of anhydrous ethanol, incubated at -80°C for 30 minutes and centrifuged at 10,000 *g* for 30-35 minutes to pellet the precipitated DNA. Supernatant was removed and the DNA pellet was dried down by speedvac. The DNA was then desalted with Amicon 30K ultrafiltration tubes according to the manufacturer's instructions and characterized by UV-VIS absorption and fluoresence spectroscopy. The DNA was then dried down, re-suspended in 10mM Tris buffer, pH~7.4 and stored in the freezer (-20°C or -80°C) until ready to use. For the AG3 sequence, a dry 1.5nmol sample

was subsequently sent to Novatia for mass spectrometry analysis to confirm its molecular weight. Secondary structures were predicted using MFold (http:// mfold.rna.albany.edu/).

2.3 Polymerase Chain Reaction (PCR) amplification procedure

PCR protocol for amplification of DNA sequences was conducted as follows. Master mix recipe per PCR reaction consisted of 50 μL of Flu-Mag Buffer, 40μL of deionized water (adjustable depending on the amount of pool template added), 8μL of 25mM $MgCl_2$, 2μL of 10mM dNTP, 0.5μL of 0.2mM Primer 1 and Primer 2, and 1μL of 500U Taq polymerase. Master mix was generally made up for 10 reactions and aliquoted in 100μL amounts into clear 0.2 mL PCR tubes. To each reaction, 5-10μL of template sample (i.e. pool DNA) was added and the tubes were placed in an Eppendorf Mastercycler thermocycler. Amplification conditions were as follows: 94°C at 5 min (for denaturation and heat activation of Taq polymerase); 20 cycles of a) 94°C 1 min, b) 47°C 1 min and c) 72°C 1 min (for annealing and extension); 72°C 10 min (for final extension); cool at 4°C (end of amplification) [81]. The samples were dried down by speedvac and resuspended to ~12-15μL volume with deionized water for loading onto PAGE. (see section 2.4 for procedure).

2.4 Denaturing PAGE protocol

A polyacrylamide gel mixture of appropriate polyacrylamide content (12% for pool synthesis and SELEX products) was prepared. Briefly, for a 12% polyacrylamide

mixture the following ingredients were combined, heated to 37°C on a hot/stir plate and filtered by gravity using filter paper (Whatman) : 23.5 mL of 30% Acrylamide/Bisacrylamide (BioShop), 31.5g urea, 15 mL of 5X TBE, 14 mL of deionized water. To this mixture 450µL of 10% ammonium persulfate solution (~0.1g in 1 mL of deionized water) and 35µL of TEMED were added by pipette, swirled briefly and poured between two assembled glass plates. 15-well combs (1.5mm) were inserted and the gel was set to polymerize at room temperature for 30 minutes. The wells were then rinsed three times with distilled water and assembled in a Hoefer SE 600 Chroma Standard Dual cooled gel electrophoresis unit filled with 1X TBE (diluted from 5X TBE stock) as running buffer. The gel was pre-equilibrated at 25mA for 15-20 minutes, during which samples were prepared with 1 equivalent of formamide and heated at 55°C for approximately 5 minutes. Samples were loaded into the wells of the gel and the unit was set to 25mA for about 1.5-2h or until all components sufficiently migrated. The current was then disconnected and the gel was transferred to a silica plate (HLF w/ organic binder, UV 254; 20x20cm; 250microns from Uniplate) wrapped in saran wrap for imaging using an Alpha Imager EC MultiImage Light Cabinet (Alpha Innotech). Images were taken under the 'epiUV' channel (for visualization of DNA absorption) and the 302nm channels (for visualization of the fluorescein label).

2.5 SELEX on Murine Norovirus (MNV)

Prior to each round of SELEX, approximately 1-2 nmol of DNA pool (~10^{13}-10^{15} sequences) in 500µL of GSB buffer was denatured by heating at 95°C for 5 minutes and

allowed to cool for 20 minutes at room temperature. A negative selection was first carried out to reduce non-specific interactions of the pool with the partitioning medium, a 0.45μm nitrocellulose filter (Millipore HAWP filters). The DNA was re-quantified to determine how much was lost. In the first three rounds of SELEX, the recovered pool was incubated with 0.5μL of 10^6 pfu/mL (approximately 500 infectious particles) of murine norovirus (MNV-1) for 30 minutes at room temperature and filtered by nitrocellulose to remove non-binding sequences. The filter was washed 1-2 times with GSB to facilitate removal of non-binding sequences which were screened in the filtrate and washes using absorbance (A_{260}) measurements. The binding complex was eluted by suspending the filter in 2-500 μL aliquots of elution buffer and heating at 95°C for 5 minutes. The binding sequences were purified using phenol-chloroform extraction followed by ethanol precipitation. The samples were desalted with Amicon Y-30K ultrafiltration tubes, as per the manufacturer's instructions. Binding sequences were checked by absorption and fluoresence whenever applicable (see Results/Discussion for details). The binding DNA was then amplified by conventional PCR using the abovementioned primers (see Section 2.3). PCR reactions were visualized on a 12% denaturing PAGE and amplified bands were excised, eluted, purified and characterized as previously described (Section 2.3). Rounds 4-7 were carried out as abovementioned with decreasing concentrations of MNV (i.e. approximately 100 infectious particles in Rounds 4 and 5; 10 infectious particles in Rounds 6 and 7). The last two rounds of SELEX, rounds 8 and 9, were counter-selection rounds with approximately 500 infectious particles of *Feline Calicivirus* (FCV) and an equivalent volume of Dulbecco's Modified Eagle Medium (DMEM). The enriched pool was amplified with unmodified primers

(Pr1u and Pr2u) for cloning in *E.coli.* Cloning was done using the StrataClone® cloning kit and isolated colonies were stabbed by pipette tip. The resulting clones were ligated into a plasmid using the TempliPhi® amplification kit (GE Healthcare) as per the manufacturer's instructions. Prepared clones were sent to University of Calgary's Core DNA Services for sequencing analysis.

3. Binding Characterization for K_D determinations

3.1 List of Materials

All measurements were carried out with a Horiba Jobin-Yvon Fluorolog spectrophotometer. Virus samples were dialyzed in GSB buffer and concentrated down before use.

3.2 Anisotropy studies on virus targets

Prior to anisotropy measurements, emission tests were conducted on test dilutions of AG3 for optimal signal at 520nm without loss in sensitivity. This was done with a Horiba Jobin-Yvon Fluorolog spectrophotometer. The lowest detectable dilution was determined to be 10^{-9}M (~1nM).

Samples were prepared as follows: AG3 sequence was prepared to 10^{-8}M (10nM) stock concentration in GSB buffer for aliquoting to mixtures with dialyzed virus/serum

stocks (MNV, GII.3, FCV, DMEM, Grace's serum). The DNA was denatured by heating at 90-95°C for 5 minutes, followed by room temperature incubation for 20 minutes. All virus stocks were prepared in 1 in 10 serial dilutions (10μL sample + 90μL buffer) with GSB buffer. 30μL of each dilution was mixed with 30μL of 10^{-8}M AG3 in an Eppendorf tube (total concentration of AG3: 5nM) and allowed to stand for an hour at room temperature. All test samples were prepared in duplicate. Single-point anisotropy was conducted on the spectrofluorometer under the following conditions: Excitation: 490nm, Emission: 520nm, slit widths: 4.00nm, Number of trials per sample: 6, Integration time: 1s. Data collected for binding curves was fitted with MS Excel, using a Hill function from which approximate K_D values were determined.

III. Results and Discussion

1. Human norovirus capsid preparation by BEVS method.

1.1 Attempts to Prepare the GII.4 capsid

Currently, the GII.4 human norovirus strain is the cause for the majority of outbreaks of non-bacterial gastroenteritis [83]. As such, SELEX was originally envisioned on this strain. Since human norovirus poses a safety risk in its handling, a non-infectious form of the virus was prepared. The capsid for the GII.4 human norovirus strain was prepared using the Baculovirus Expression Vector System described in Section 2.1 (see Introduction). The transfer vector PVL1393 contains an insert that codes for VP1 of the GII.4 strain, which is the region of the norovirus genome that corresponds to the viral capsid. This was co-transfected with Bacculovirus DNA in *Sf9* cells, to form a recombinant baculovirus and commence infection of the cells. Figure 12 shows a sample of observations from a third-passage (P.3) amplification that indicates the presence of an infection. Control plates were conducted in parallel for comparison: A negative control represents no infection whereas a positive control demonstrates an infection with a wild-type bacculovirus called AcNPV. Healthy *Sf9* cells have uniform size, adhere to a surface (e.g. a tissue culture plate) to form a monolayer and double every 18-24 hours. Infected cells appear enlarged, disfigured, have enlarged organelles (i.e. vacuoles and nuclei), float in solution or attach poorly to a surface, and cease dividing. Polyhedrin proteins, which coat wild-type baculovirus particles to confer environmental resistance and viral stability, may also be visible late in an infection (usually 3 days post-infection).

However in recombinant baculovirus, these polyhedra are not visible because the gene is non-essential to virus replication and is typically replaced by the inserted gene.

The virus stock was harvested and a plaque purification assay was conducted to reduce the likelihood of unwanted mutated forms of the baculovirus propagating. When each infected cell produces virus and eventually lyses, only immediate neighbouring cells get infected and are surrounded by uninfected cells. Each group of infected cells (referred to as a plaque) represents a single infection (i.e. a virus particle). When light passes through the infected cells, it refracts differently than it would in uninfected ones and can be easily identified, appearing as round voids in the cell monolayer. Nine plaques potentially containing the recombinant virus were isolated. The samples were eluted from the plaques and amplified twice. They were then qualitatively screened by SDS-PAGE (Figure 13) for the presence of a ca. 60kDa band, corresponding to the molecular weight of the capsid protein VP1. Of the 9 candidates tested, two samples (VL-1 and VL-3) appeared promising and were continued with BEVS. This was based on faint signs of the 60kDa band, which may be attributed to the two-fold amplification yielding a relatively low titer ($\sim 10^3$ pfu/mL). It is also noted that two candidates (VL-6 and VL-8) were discarded from the characterization, due to a fungal contaminant observed in only these two samples. With subsequent amplification and plaque assay quantifications, the titer appeared to gradually increase (Table 1). Usually these plaques were easily identified without staining but in particularly challenging instances, 0.1% crystal violet staining was attempted as a last resort. However, it did not provide any further visualization of the

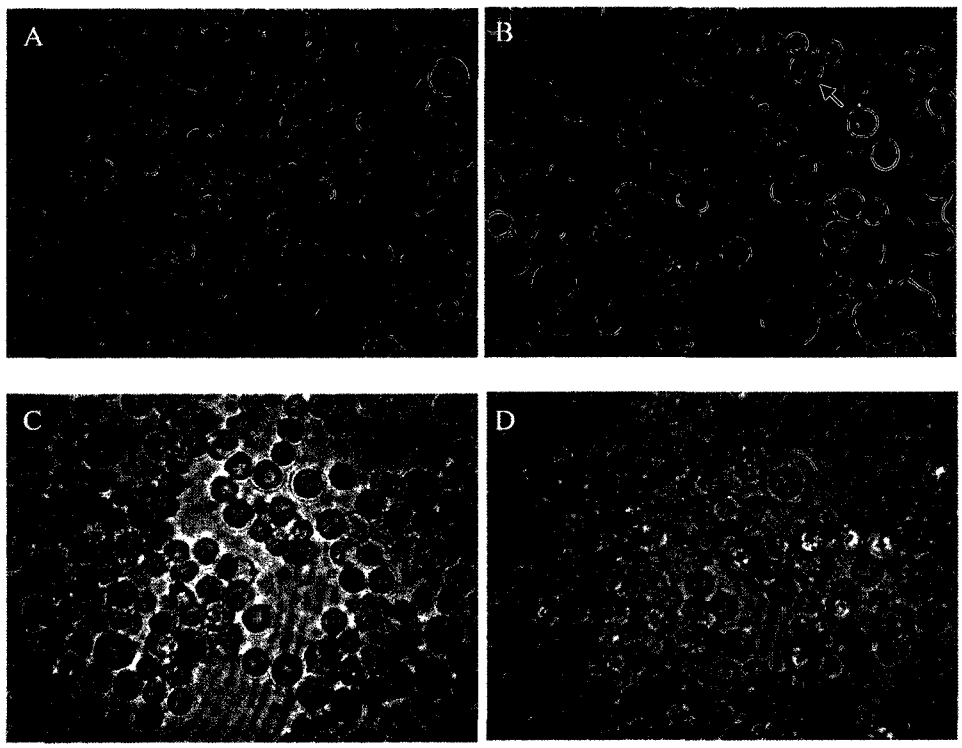

Figure 12: Observations of *Sf9* cells in a passage three (P.3) amplification of recombinant baculovirus. MOI ~0.01 and images were taken 6-7 days post-infection. A: negative control, B: positive control (AcNPV), C: VL-1, D: VL-3. Polyhedrin protein is observed in the positive control (arrow).

plaques and tends to be a more fastidious procedure. Crystal violet staining requires the removal of the agarose plug by treatment with 4% para-formaldehyde and then gentle dislodging of the plug with pressure (in this case it was done by applying water to the plug to push it out), followed by the actual staining. However, this introduces the risk of destroying the cell monolayer and can skew plaque counts. A staining process that mimics a standard cloning protocol to produce colour-coded colonies would be a means

of improving on the method to provide a more accurate titer. This would be possible if one uses a modified version of AcNPV that contains the LacZ gene (e.g. AcRP23.lacZ), which gives off blue coloured colonies, when reacted with X-Gal treated agarose [22]. This way, colonies containing the gene of interest (i.e. lacking the lacZ gene) can be more easily screened and counted.

During the amplification stage of BEVS, steps were taken in attempts to improve the probability of infecting the cells and obtain higher recoveries of the virus. For instance, incubation times were extended from the standard 3-5 days to 6-7 days to allow a more thorough infection cycle as earlier shown in Figure 12. The MOI was also adjusted to a lower value (~0.01) since low MOI passage (< 0.1) prevents an increase in the amount of virus with extensive mutations in the genome. Eventually, a viral titer

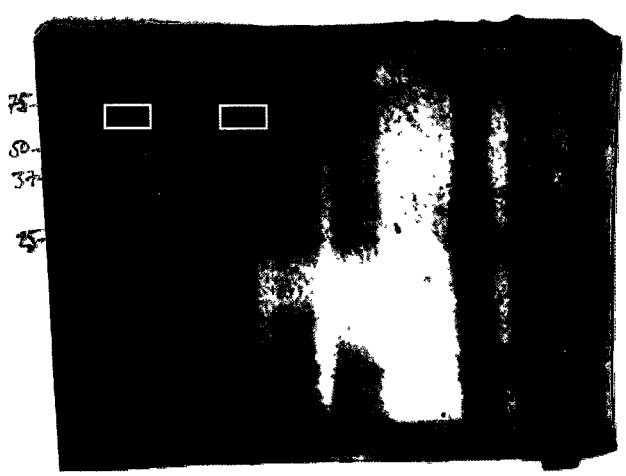

Figure 13: SDS-PAGE characterization for presence of GII.4 capsid candidates (L to R) kDa Protein Ladder, VL-1, VL-2, VL-3, VL-4, VL-5, empty lane, VL-7, VL-9, -ve ctrl. Candidates VL-6 and VL-8 were discarded due to a fungal contamination.

assessed to be ~10^6 pfu/mL was used for protein expression (Figure 14). Although this was still two orders of magnitude shy of the recommended titer of ~10^8 pfu/mL, it was calculated to suffice for a small-scale protein expression and find out if the samples showed any potential. A high MOI was used (MOI~4) for protein expression and the incubation time was limited to three days since prolonged incubation would increase the chance of mutant proteins being expressed. Minimal signs of infection were only observed and the supernatants of the samples were harvested and characterized by SDS-PAGE to check for signature bands. Comparisons were made to a few extra markers: MB40, W2 and 809, all of which are GII.4 strains from various imported stool samples, as well as the protein ladder. It appeared that no bands corresponding to the 60kDa mark were observed (see Figure A2 in Appendix for images). Furthermore, the AcNPV sample was expected to contain a 29kDa band, corresponding to the polyhedrin protein which also did not appear in the sample.

Viral passage	**Approximate titer of VL-1 (pfu/mL)**	**Approximate titer of VL-3 (pfu/mL)**
P.1 (amplification, pre SDS-PAGE)	10^2	10^3
P.2 (amplification, post SDS-PAGE)	10^3	10^4
P.3 (amplification)	10^4	10^5
P.4 (amplification)	10^6	10^6

Table 1: Summary of observed titer for virus amplifications of candidates VL-1 and VL-3 based on plaque counts.

Further troubleshooting for the experiment was attempted in order to recover the capsid. A previously amplified stock of GII.3 capsid was included as an additional positive control and the incubation time was extended to a maximum of 4 days. Observations showed some signs of infection and the resulting SDS-PAGE characterization on the harvested supernatant (i.e. secreted protein) demonstrated the presence of the GII.3 capsid at the approximate 60kDa area (Figure 15, lanes 8 & 9). It was still possible that the capsid may have been present in the VL-1 and VL-3 samples (lanes 12 & 13) as dense regions in the lanes were noted, however, it seemed that some of the loading dye (likely due to a run condition) simultaneously obscured these observations rendering them indeterminate. Another possibility that was addressed was that perhaps the protein had not yet secreted into the supernatant and may in fact have still been inside the cells. Thus, the protein expression experiment was retried at an incubation time of 4 days, resulting in the same infection observations (Figure A3 in Appendix). This time, both supernatant and cell pellet were characterized by SDS-PAGE. The GII.3 capsid tested positive in both sample types with most protein secreted from the cells. The VL-1 and VL-3 (Figure 16) samples still did not show a capsid band in either the supernatant or cell pellet. Similar observations were found for AcNPV indicating that either the virus was not present and resulted in a failed protein expression or had relatively poor expression levels.

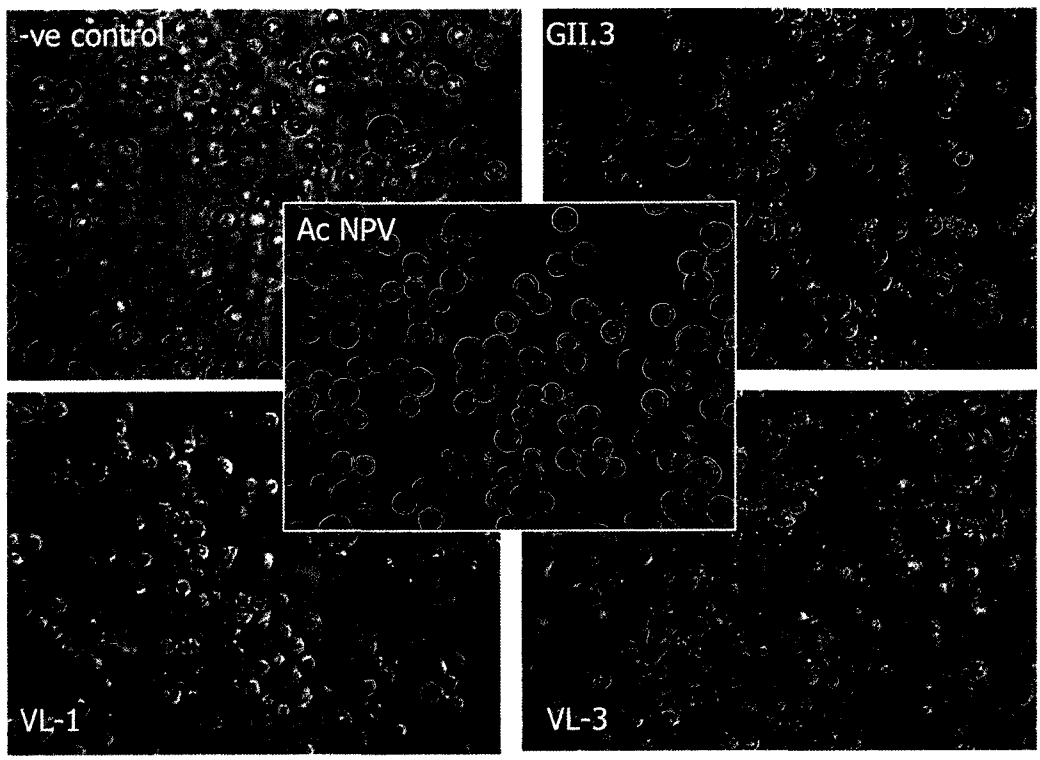

Figure 14: Observations of Protein expression experiment #2 (MOI~3, t = 3 days).

Figure 15: SDS-PAGE characterization of protein expression experiment #2. Sample-containing lanes are as follows: 2-1Kb LADDER; 4- 809 (+ve); 5-MB40 (+ve); 6-W2 (+ve); 8, 9-GII.3 capsid; 11-AcNPV (+ve); 12-VL-1; 13-VL-3; 14-negative control (supernatant from cell culture).

There are various biological interferences that can impact the progression of this expression system. One possibility is that even though signs of infection were present, the baculovirus may have been expressing something other than the preferred capsid. This could have occurred during plaque pickup where co-expression of mutant baculovirus (containing deletions, substitutions or additions to its sequence) is possible. For instance, the PVL1393 vector used in BEVS contains a polyhedrin promoter. Polyhedrin is a major component of the outer protein shell of the baculovirus, providing resistance to hostile environmental conditions and thereby contributing to its stability in the host. The polyhedrin promoter in PVL1393 is common to AcNPV but lacks part of the polyhedrin gene coding region that is non-essential for replication and instead accommodates the foreign insert. A point mutation (i.e. nucleotide sequence modification) in the promoter region of PVL1393 could reduce levels of messenger RNA (mRNA), which would consequently affect the protein yield.

Defective interfering particles (DIPs) [84] are another possible factor in this procedure. DIPs are a consequence of multiple passages of virus stock. These particles have a large (up to 40%) portion of their genomic DNA deleted which can include the foreign insert. Consequently, DIPs cannot propagate autonomously causing the protein expression levels to drop with serial passage (Figure 17). Although typically this effect is reduced by infections at low MOI, it might not be completely eliminated as a potential interference.

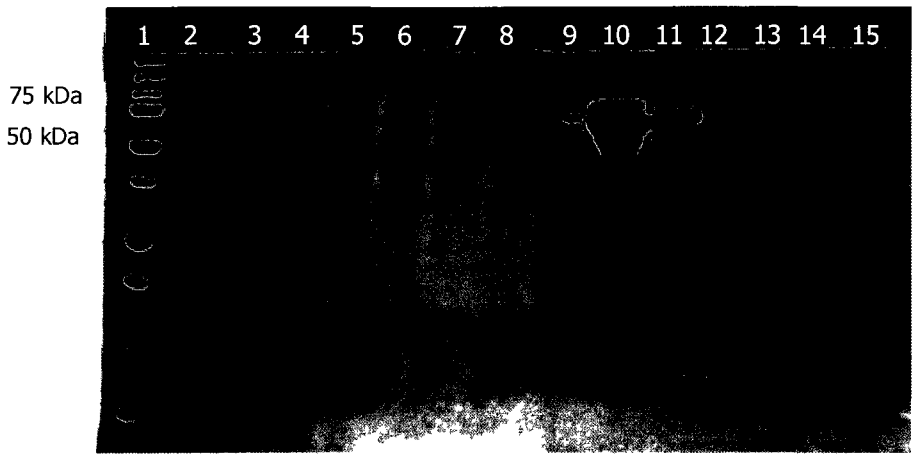

Figure 16: SDS-PAGE for protein expression experiment #3. Lanes are as follows: *1*- 1Kb LADDER; *2*- cell culture supernatant (-ve); *3*-cell pellet (-ve); *4*- VL-1; *5*- VL-1 (cell pellet); *6*- VL-3; *7*- VL-3 (cell pellet); *8*- AcNPV; *9*-AcNPV (cell pellet); *10*-GII.3; *11*-GII.3 (cell pellet); *12*-MB40 (+ve); *13*- W2 (+ve); *14*- 809 (+ve); *15*-serum-free media (blank sample)

Other possible interventions could occur during post-translational modifications of the protein. Essentially these are chemical modifications that take place following protein synthesis that adds functionality to the protein such as folding, stability, and transfer to various organelles. If for instance an amino acid is improperly oriented or in the wrong order, protein expression cannot be completed and may result in a failed expression.

Technical aspects of BEVS also affect the outcome of the expression. For instance, cells that are continuously passaged for more than 6 months can result in reduced protein production as well as the efficiency of the production [22]. Although low

passage cell stocks (< P.10) were used out of liquid nitrogen storage, it may have still not been sufficient to override this effect. Another cause for barely visible plaques, and the infection in general, is if the seeded cells were too dense. Confluency would be reached sooner and inhibit virus replication which would mask signs of infection. Though it did not appear that the cells were over-seeded and thus overgrown, they were observed to be quite confluent in most cases and may have overshadowed any infection symptoms. Thirdly, as earlier mentioned, a sufficient viral titer is a key factor in the efficiency of BEVS. Since the titer assessed had overall low results and based on the findings of the gels, the viral dilutions inoculated may not have yielded visible plaques. Short incubation time can additionally contribute to an absence of plaques. In conducted plaque assays, incubation times were extended up to 10 days, when plaques were not yet visible after the minimum period of 6 days.

Although time constraints limited this particular experiment, optimization can be attained to improve the experiment for enhanced monitoring of the expression. For example, since protein formation is a result of translation from RNA, one may attempt to detect the RNA (specifically messenger RNA) levels using Northern blot hybridization. This involves an RNA gel transferred to a membrane and then hybridized with labelled probes for a measureable detection (e.g. fluoresence, radioactivity, etc) [85]. Another approach for optimization can be achieved by introducing a stain called 'neutral red' [86] in the agarose solution. This would improve plaque visualization by preferentially staining healthy cells and leaving infected cells white and also avoiding extra steps such as dislodging the plaques which could risk destroying the cell monolayer. Other means of

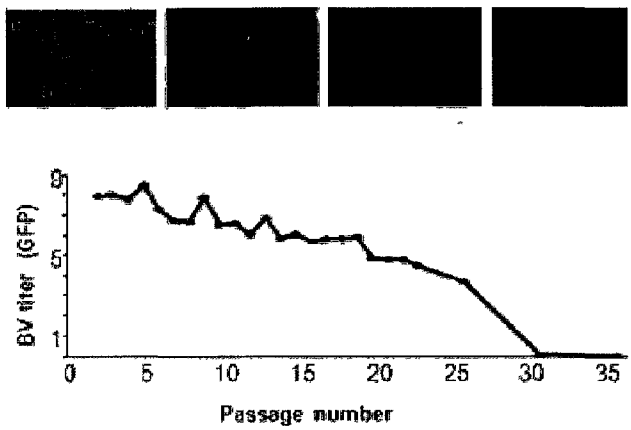

Figure 17: Effect of increasing passage number on baculovirus titer monitored here by Green fluorescent protein (GFP). [84] (Reproduced with permission from Elsevier.)

optimizing the process includes conducting the protein expression at various MOI's and then running the supernatants on SDS-PAGE to determine which expression results in the most protein produced.

1.2 Preparation of GII.3 capsid

In replacement of GII.4, the GII.3 capsid was amplified and expressed for later use in validation studies with aptamers. GII.3 is another strain of human norovirus that is very similar in structure to GII.4 with a capsid amino acid identity range of 56-86% [34], thereby making it a relevant target for this study. A previously cultured P.2 stock (~10^7 pfu/mL) was used to amplify the virus at an MOI of 0.25. The corresponding positive control from these virus stocks was used, called XylE-PVL1392 (herein called "XylE"). XylE refers to a control recombinant baculovirus that can be used as an alternative to the wild-type control for confirmation of infection. The signature band of the XylE control is a recombinant protein of 40kDa in size. Unlike the wild-type virus AcNPV, this baculovirus does not express polyhedrin. Signs of infection were minimal after three days of incubation and only slightly improved after 5 days with more floating cells and enlarged cells observed (Figure 18). The titer was assessed by plaque assay to be ca. 2 x 10^8 pfu/mL for GII.3 after 7 days of incubation and remained unchanged after extending to 10 days. For comparison, the XylE titer was assessed to be 5 x 10^5 pfu/mL and no signs of polyhedrin protein were apparent.

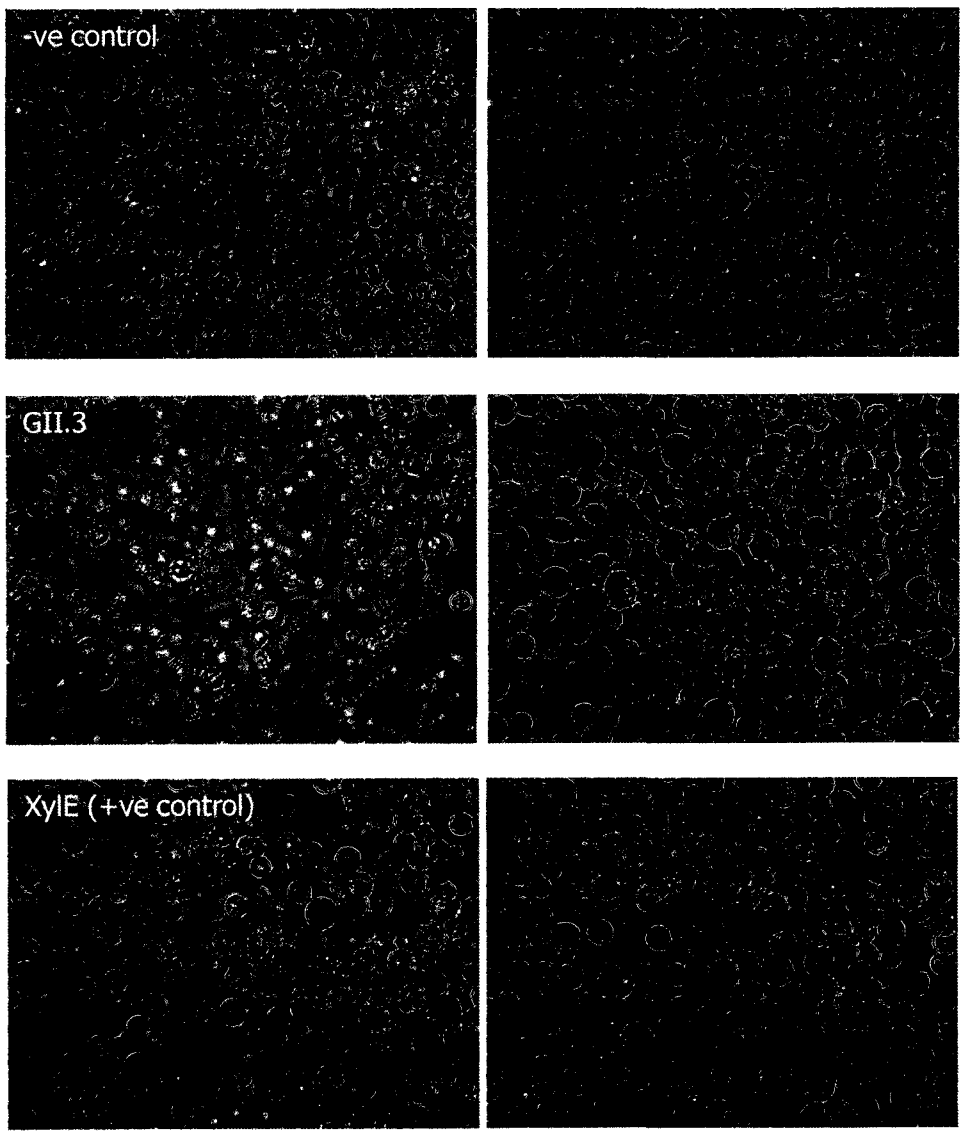

Figure 18: GII.3 BEVS P.3 amplification observations for signs of infection 3 days and 5 days post-infection.

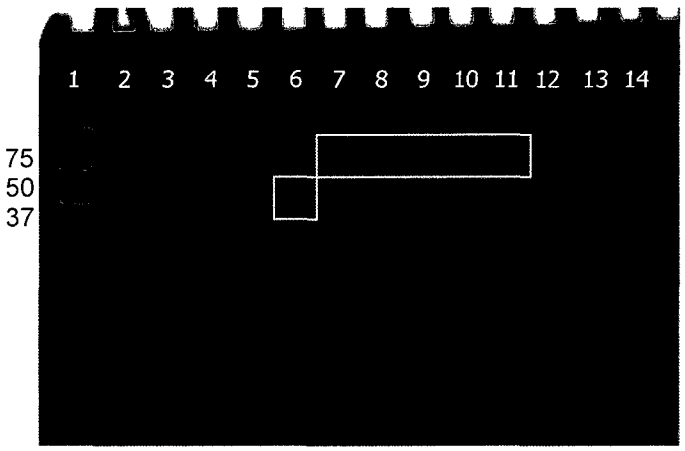

Figure 19: SDS-PAGE characterization on expressed GII.3 capsid. 1-LADDER; 2-809; 3-MB40; 4-W2; 5-XylE; 6-XylE (cell pellet); 7-MOI~8; 8-MOI~8 (cell pellet); 9-MOI~6; 10-MOI~6 (cell pellet); 11-MOI~4; 12-MOI~4 (cell pellet); 13- negative control (supernatant from cell culture); 14-negative control (cell pellet).

Protein expression for GII.3 was tested at MOI's of 4, 6, and 8 showing signs of infection and the expression of secreted protein was confirmed by SDS-PAGE (Figure 19) against ladder and virus controls. Cell pellets of each MOI were also run for comparison and showed that while some protein remained inside the cells, more protein had secreted into the supernatant. For the XylE control, a more intense band is observed in the cell pellet between 37 and 50kDa which may be the 40kDa protein, and may imply that the protein had not yet secreted into the supernatant. Interestingly, the supernatant controls showed a slight contamination but since these bands were considerably lower in intensity than in the experimental samples, it was suspected that the contamination was not pertinent. Another notable observation is in the comparison of the secreted protein in lanes 7, 9, and 11 to the GII.4 controls (MB40, W2 and 809). The GII.3 secreted protein

appears slightly higher than the GII.4 bands. While all bands compare between the 50 and 75 kDa limits, their exact masses cannot be distinguished in this region. It is postulated that the amino acid differences between strains could be a contributing factor in this discrepancy. Also, any post-translational modifications (e.g. functional groups from simple molecules to complex carbohydrates) that took place may have also added molecular weight to the recombinant product. The post-translational modifications reported to occur in BEVS include glycosylation, phosphorylation, acylation, carboxymethylation and peptide cleavages. Native norovirus particles are not known to undergo post-translational modifications [87] but with a lack of cell culture system for this virus, this remains to be absolutely confirmed. With the presumption that it does not, this may compensate for the size differences. Alternatively, it has been observed that norovirus may be cleaved by its hosts' protease (an enzyme that breaks peptide bonds in a protein) to generate soluble capsid protein while assembled capsid (i.e. capsid that was cultured) cannot be cleaved [88] and may describe this difference in the samples.

Finally, in order to reduce non-specific interactions in later experiments with aptamers, the supernatants at each MOI were purified to isolate the capsid from other cellular debris that was present. These samples were then used to characterize the aptamers that were selected against MNV (Section 3).

2. SELEX for human norovirus using MNV model.

As previously mentioned, the initial objective was to conduct SELEX on a human norovirus strain. An additional possibility of a toggle selection with the human strain and an animal strain known as MNV was also envisioned in which SELEX is alternated between multiple targets to obtain aptamers that could interact with both targets. Since the human virus strain was not obtained in time to start a SELEX experiment, an aptamer selection on MNV was conducted with the later incorporation of the human strain, GII.3, in aptamer characterizations (see Section 3). MNV was chosen as a SELEX target since it is often used as a model for human norovirus. As described in section 2.3 (see Introduction), MNV shares similar structural characteristics to human norovirus and since it can replicate in cell culture, it can provide good insight into human norovirus behaviour.

Negative selection was first conducted against a nitrocellulose filter, which acted as the partitioning medium in the SELEX experiment which removed sequences from the starting DNA library that would have a non-specific interaction with the filter. About 1.6 nmol (~ 1 x 10^{15} sequences) was passed through the filter with a recovery of about 1.1 nmol (68% of the initial pool). Positive selections then followed using MNV-1 (hereafter generally referred to as 'MNV'), which was previously dialyzed in general selection buffer (GSB). About 500 infectious particles of MNV was decided as the starting concentration of target for the first round of SELEX. Since DNA and protein are generally capable of intermolecular interactions with one another, a small amount of

target was used to create a highly competitive environment for the DNA library such that only sequences with a very strong affinity could survive the selection. Additionally, this amount was observed to retain on the filter without any sample loss during filtration. This stringency was increased (i.e. decreasing target content to 100 and 10 infectious particles) at various points in the SELEX rounds to achieve a strongly binding pool. Figure 20 summarizes the observations of the SELEX experiment conducted on MNV. In the first three rounds, a net increase in the amount of retained sequences was observed, supporting the enrichment of the DNA pool from one round to another. As stringencies of 100 and 10 infectious particles were introduced in subsequent rounds, the amount of retained sequences initially dropped and then increased drastically in following rounds as expected. In the last two rounds, counter-selections were conducted to account for non-specific interactions with similar or analogous compounds that mimic MNV or might be mixed with MNV in a real sample. FCV is such an example since it derives from the same family (*Caliciviridae)* as norovirus but belongs to a group called *Vesivirus* which has slightly different structures. While MNV and human norovirus capsids share a spherical appearance under electron microscopy, FCV capsid appears more hexagonal in structure [89] which may be related to differences in amino acids of the P domain. A counter-selection was completed with 500 infectious particles of FCV and the recovery of this round is reported in Figure 20 representing DNA that did not interact with the counter-target. A second counter-selection was followed with a serum called DMEM, which was previously used for culturing MNV in the laboratory. The serum contains a variety of vitamins, amino acids, inorganic compounds and other salts [90] thereby making this counter-selection significant to remove non-specific interactions. For consistency, an

aliquot of DMEM was dialyzed in GSB before counter-selection with the round 8 pool. Consequently, some of the components in the serum, particularly the smaller compounds, may have already been removed during the dialysis since the procedure is essentially a dilution process in which equilibrium between a volume of sample and a relatively large volume of exchange buffer takes place. A large, comparable recovery of the pool in rounds 8 and 9 indicated that the pool could be favouring MNV over these other two counter-targets.

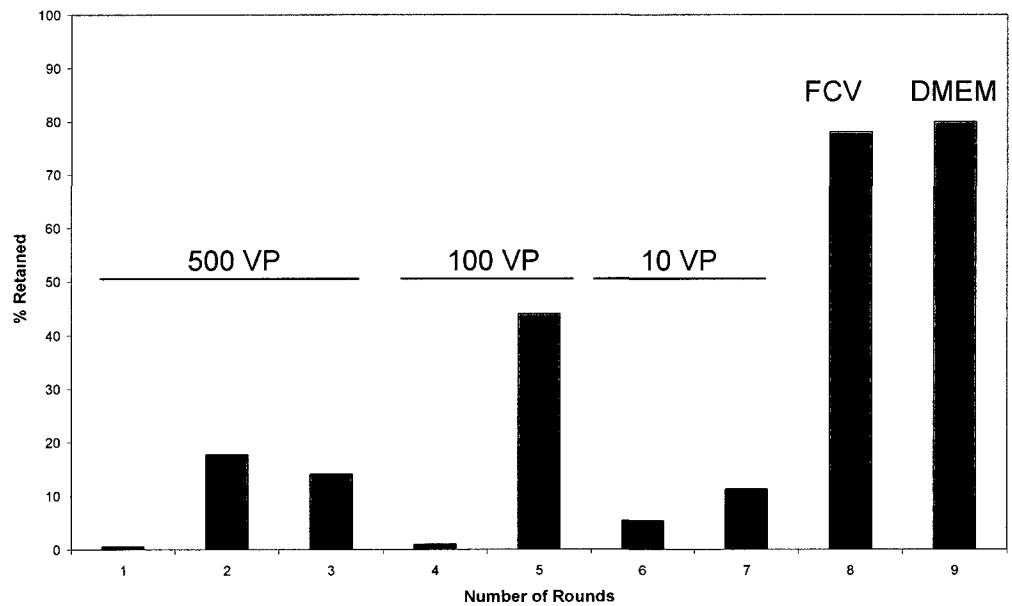

Figure 20: Summary of rounds for MNV SELEX. Target concentrations are outlined for sets of rounds. Retained fractions were assessed, based on loss of non-binding sequences during partitioning. Counter-selection rounds 8 and 9 are an actual measure of the pool, since this was DNA that did not interact with the indicated targets (i.e. passed through partitioning).

Undoubtedly, there were some particular challenges during the selection experiment. During elution, heat and a urea-based buffer were used to ensure that the retained DNA was completely removed from the filter. Purification procedures (i.e. phenol-chloroform extraction and ethanol precipitation) proceeded as usual, however when the samples were checked following the desalting step prior to amplification (section 2.5 in Experimental Methods), distinguishable signals were observed in the filtrates at ~λ= 265nm (figure A4, red and green signals). To ensure that DNA was not lost to the desalting tube, a PCR test amplification was conducted to look for "contamination" (Figure 21). The PCR result was negative for these filtrates but positive for the recovered sample. It was found in the literature that urea can cause the capsid to denature by disrupting hydrogen bonding and disrupting van der Waals interactions [91]. Consequently, this can release the RNA genome into the solution. Based on these observations, it seemed that RNA might have been the candidate for the filtrate signals since RNA cannot be amplified by the PCR enzyme, Taq polymerase. However, since the phenol-chloroform was buffered at pH~8, it preferentially isolates DNA in the aqueous phase, and RNA and proteins in the organic phase [92]. Perhaps some of the interface was drawn out when the aqueous phase was extracted by pipette and then separated out during precipitation and desalting procedures. When the recovered samples were screened for DNA by absorbance, signals were observed around the λ~ 257nm mark (Figure A4 purple signal, and A5 in Appendix) and quantifications were within range compared to the amount determined, based on the loss of DNA during partitioning. Another difficulty encountered was that fluoresence measurements lacked sensitivity for direct

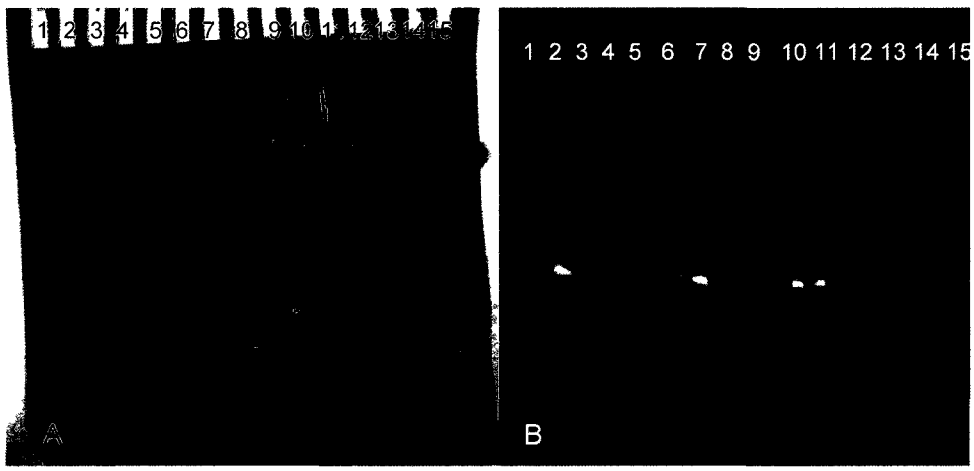

Figure 21: Denaturing PAGE gel of Round 1 PCR test amplification on retained DNA pool. Sample lanes are as follows: 2, 10-negative control; 7, 11-positive control (1 in 10 000 dilution); 3-5-retained DNA pool; 6-desalting cleanup (filtrate). Image A was visualized under UV shadow and Image B is imaged under fluorescent channel.

quantification. The fluorescein modification would allow for distinction of binding DNA against all other components in solution, however, measurements of these samples proved challenging for various reasons. In some cases, the recovery volumes were too small or too dilute for a measureable signal and concentrating the samples down would have resulted in insufficient volumes for sample measurements. It is also possible that the fluorescein modifier may have been photo-bleached at some point during the selection. Since fluorescein is light-sensitive, working under high illumination conditions can limit fluoresence intensity [93]. Photobleaching by oxygen in solution is the most common way and can occur on most fluorophores, producing a radical species that is non-fluorescent. At large-scale concentrations, this effect under working conditions is negligible but at lower concentrations, it is likely more noticeable. Organic extraction components were also searched for fluorescein to no

avail (Figure A6, Appendix). Regardless, the modifier was regenerated upon PCR amplification via the tagged primer, allowing for easy detection and isolation of the amplified aptamer pool in each round (see also Figure A7, Appendix). For these abovementioned reasons, it was more convenient to determine the amount of DNA retained as summarized in figure 20, based on the observed loss of non-binding sequences during partitioning.

Figure 22 is an example of typical observations of PCR amplification (in this case, shown for Round 7). As earlier discussed (see Chapter 3 of Introduction), two differently modified primers were used for easy separation of all PCR components. The fluorescein-modified primer (Pr1) would amplify the aptamer pool and the A_{20}-HEGL modified primer (Pr2) would amplify the complement. Since Pr2 is a heavier sequence than Pr1, the pool would migrate further in PAGE than would the complement sequence. Along with the standard PCR negative and positive controls, various other controls were incorporated to demonstrate that sequences from the stringent selection were being retained. These include filtrate samples post-desalting and an MNV control selection sample (a selection in which no pool was added). Both confirmed that they were neither contaminated nor contained amplifiable components that would interfere with the selection. Another notable observation that recurred starting with Round 5 is that a second set of faster migrating bands had started to amplify and survived the remainder of SELEX. For this reason, these bands were recovered and incorporated for the remainder of the selection, to determine if they contained potential strands or if they would end up partitioned out in the selection.

Following cloning and sequencing results, three potential aptamer candidates were found, which are summarized in Table 2 with predicted secondary structures represented in Figure 23. Out of 40 total clones, one sequence (AG3) was found to recur ten times, with a slightly truncated random region of 33nt as well as a truncated primer region at the 3' end. This could have been caused by some non-specific priming in PCR where the primers can anneal to repeat sequences in the template, non-specifically bind to the template and/or incompletely bind to the template. Nonetheless, it was still of interest to investigate this candidate as it was common to both amplified bands observed and it is not completely implausible that this could have been a coincidental occurrence in the selection. Two other clones (AG28 and AG29) were identified with only one occurrence of each but maintained their 40nt random region and primer regions. These were comparably different from each other with only 12 conserved nucleotides in the random region. Secondary structure predictions show bulge and hairpin features common to all three candidates as the lowest energy conformation. The bulge regions might represent binding pockets that interact with the capsid. It is important to note that these structures do not account for G-quadruplex formation, which was a possibility that stems from observations of the pool's ultraviolet absorbance. In comparison to the original library absorbing at 260nm, the amplified pool was found to exhibit a shifted wavelength at around 256nm. A maximum absorbance of 260nm is the average wavelength for DNA, assuming a relatively uniform combination of the nucleotide bases. However, if there is a bias towards a particular nucleotide, the maximal absorbance shifts towards the wavelength of that nucleotide. Since guanine has a maximum absorbance at about

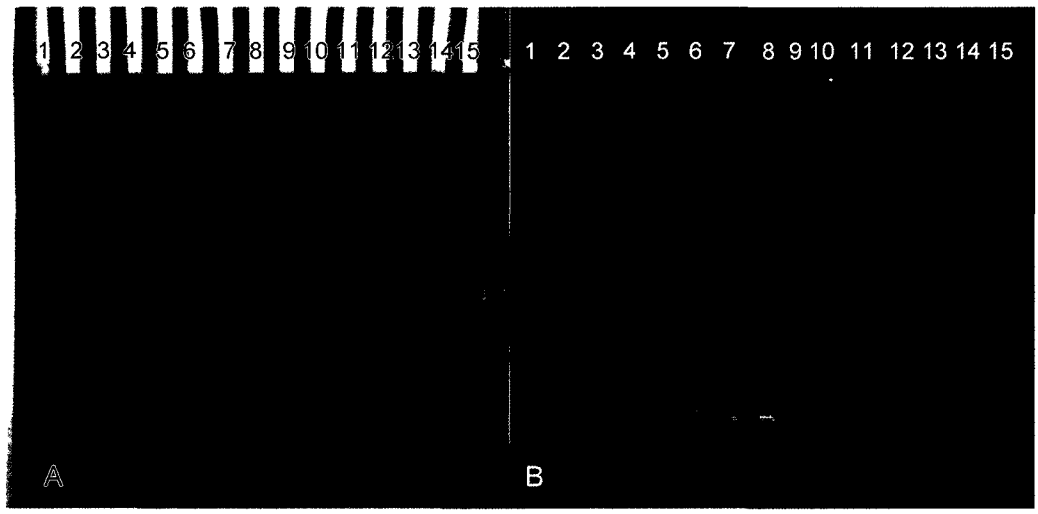

Figure 22: Denaturing PAGE of Round 7 PCR amplification observations under UV channel (A) and Fluorescent channel (B). 1-3: negative control, 4: MNV control, 5-8: filtrate, 9&10: positive control (initial DNA library), 11-15: MNV subjected to DNA pool.

Name	Sequence	G content
AG3 (10)	GCTAGCGAATTCCGTACGAAGGGCGAATTCCACATT GGGCTGCAGCCCGGGGGATCC	33%
AG28 (1)	CGTACGGAATTCGCTAGCACGGGGCTTAAGGAATAC AGATGTACTACCGAGCTCATGAGGATCCGAGCTCCA CGTG	29%
AG29 (1)	CGTACGGAATTCGCTAGCCGACGGTCAATGCTCGTG AGCCAGTACACACAATATATGTGGATCCGAGCTCCA CGTG	26%

Table 2: Summary of aptamer candidates (read 5'→3'). Candidate names refer to the name of the isolated clones. The number in parenthesis represents the frequency of the individual clone. Underlined sequences represent the primer regions.

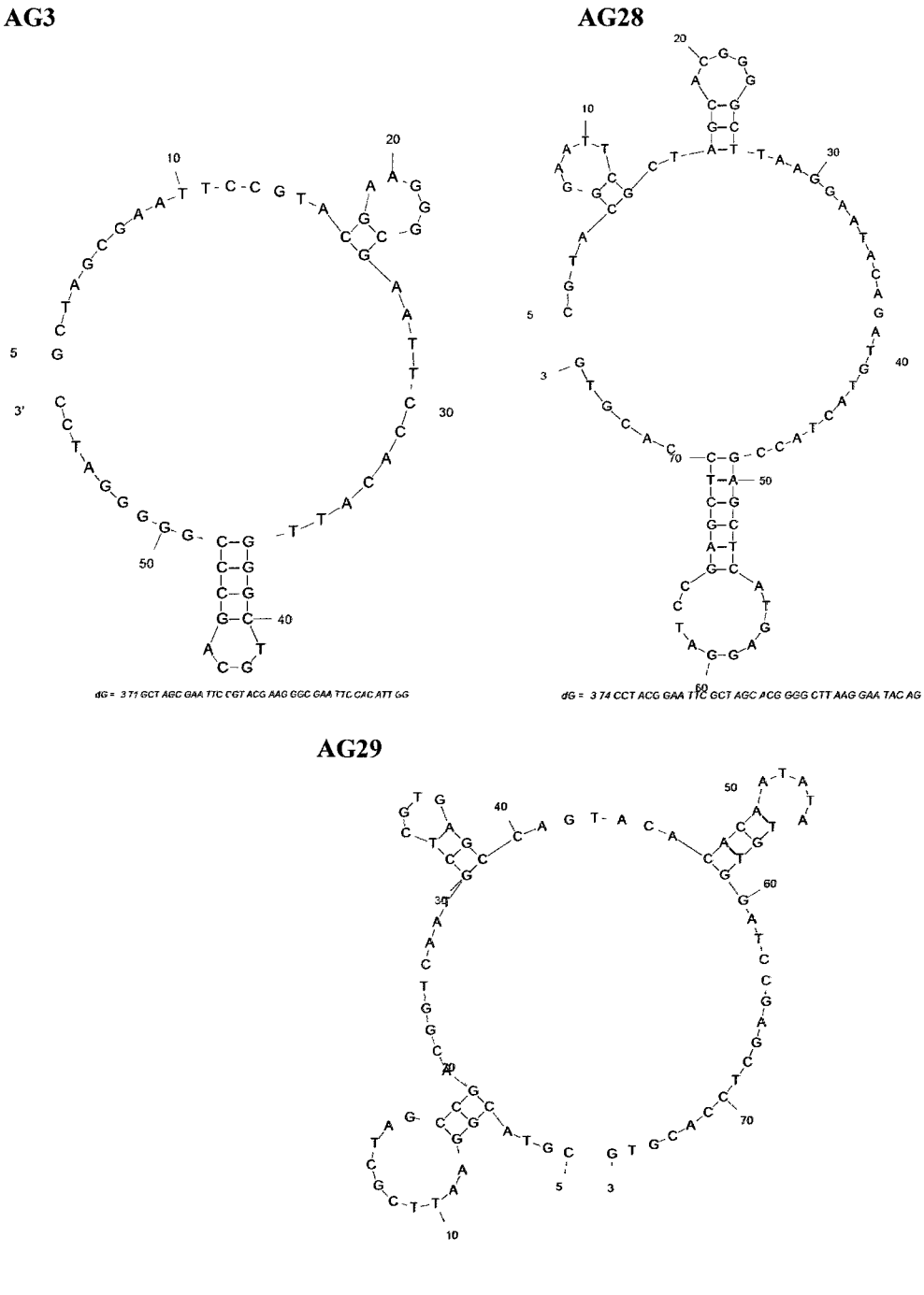

Figure 23: MFold secondary structure predictions of aptamer candidate sequences showing stem-loop and bulge features.

252nm [94], it is possible that the pool was enriching with more G-containing sequences and causing a blue-shift in the maximum absorbance. Indeed, guanine is found to be the most abundant of the nucleotides in the AG3 sequence. A QuadFinder [95] analysis showed potential for G-quadruplexes mostly in regions shared by the random region and the primer region (see figure A8 in Appendix). Therefore, it is possible that the primer regions contribute to significant binding features of these sequences.

3. Binding studies for aptamer candidate AG3.

With regards to binding characterization, AG3 was primarily studied since it had the highest clone occurrence and thus may have had the most affinity for MNV among the identified candidates. Fluoresence anisotropy was chosen as the affinity experiment for determining the sequence's dissociation constant (K_D). Since the aptamer and target have a significant mass difference, a signal change could be detected in this method. Figure 24 shows the binding curves of various test targets at different concentrations, with a constant concentration of AG3 candidate. Binding curves were constructed with Excel and fitted using a Hill function (see section 4.2 of Introduction), which is typically used to describe protein-nucleic acid interactions. Assessment of the fit to the experimental data is also included (insets of Figure 24) with calculated R^2 values found to be close to 1, demonstrating a good fit between experimental and theoretical values. Among the targets studied, AG3 showed the highest affinity for MNV with an estimated K_D of about 5.3×10^{-14} M. Solving for coefficients that describe number of interactors (n) and the degree of cooperativity (α_H) for this fit, resulted in values of 1 and 1.47 respectively, indicating that mainly non-cooperative binding (i.e. $\alpha_H \sim 1$) was favoured. This may imply that the binding sites on the MNV capsid are similar which coincides with its repeating monomer protein.

For the GII.3 capsid (Figure 24, B), the K_D value was challenging to estimate, due to the limitation of its stock concentration. Consequently, it cannot be certain that saturated binding is complete. The theoretical fit shown here predicts a K_D at around

7×10^{-13} M, assuming that saturated binding is achieved. If this is indeed the case, affinity for GII.3 would be one order of magnitude weaker than that for MNV. Although one would expect that the capsid should bind with similar affinity to the MNV capsid, this discrepancy could be related to differences in the P2 region of the capsid. Since P2 is the most variable region of the virus, especially between species of norovirus, differences in amino acids or its orientation could contribute to a difference in binding affinity. This is not unexpected as MNV was the sole target of the selection and so it is anticipated that the generated aptamer candidate will have a more favourable affinity for that target. Had the GII.3 capsid been more readily available, Toggle SELEX would have been introduced, where one alternates selection rounds with two targets to yield aptamers that can detect them both [96] and perhaps obtain more similar K_D values. Even so, the affinity of this aptamer candidate for this virus appears to be low compared to those for other pathogenic targets. For example, aptamers selected against the internalin A protein of *Listeria monocytogenes* has a reported K_D of 84nM, while egg-white lysozyme, an allergen trigger, has a reported K_D of 3nM [69]. Another factor is that there may be some non-specific interaction with culture components in the GII.3 sample that perhaps were not completely removed from purifications. A slight signal change with both sera—DMEM for MNV and Grace's Insect Media for GII.3, was observed at the lowest dilution (Figure 24 D) which provides a small chance of non-specific interaction but less probable as an influence since the virus targets were dialyzed in selection buffer.

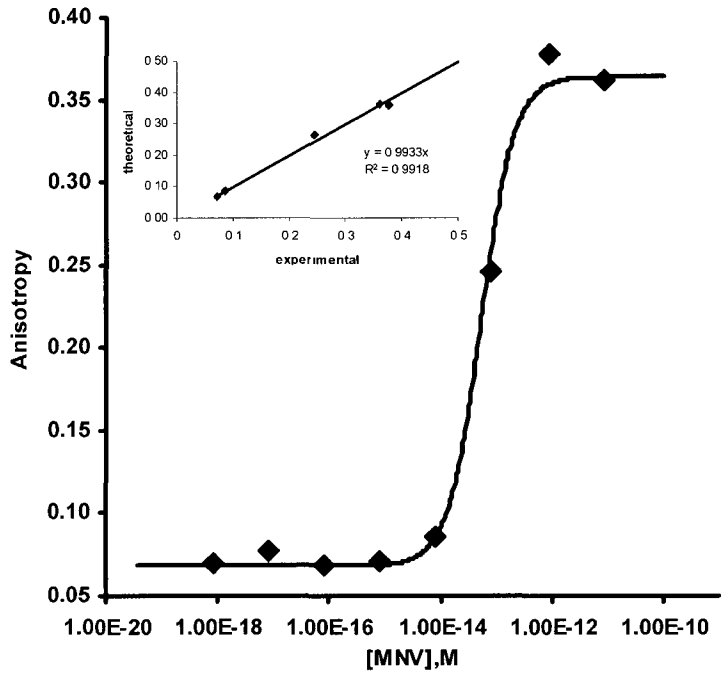
0.40
0.35
0.30
0.25
0.20
0.15
0.10
0.05
Anisotropy
1.00E-20
1.00E-18
1.00E-16
1.00E-14
1.00E-12
1.00E-10
[MNV],M
theoretical
experimental
y = 0.9933x
R² = 0.9918

A

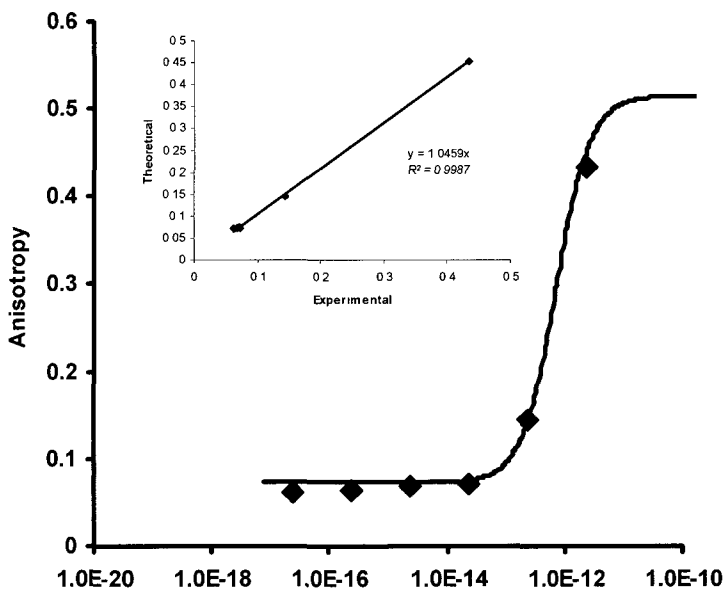
0.6
0.5
0.4
0.3
0.2
0.1
0
Anisotropy
1.0E-20
1.0E-18
1.0E-16
1.0E-14
1.0E-12
1.0E-10
[GII.3], M
Theoretical
Experimental
y = 1.0459x
R² = 0.9987

B

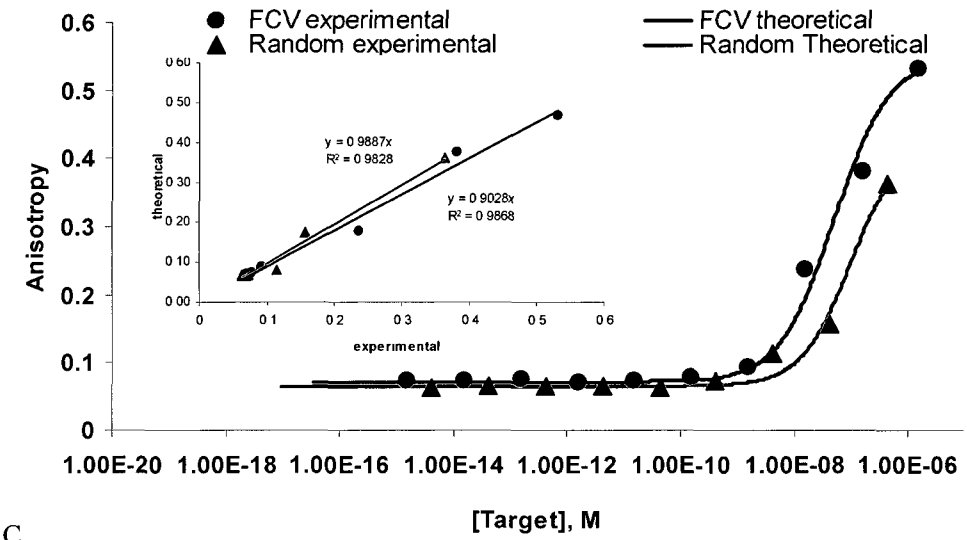

C

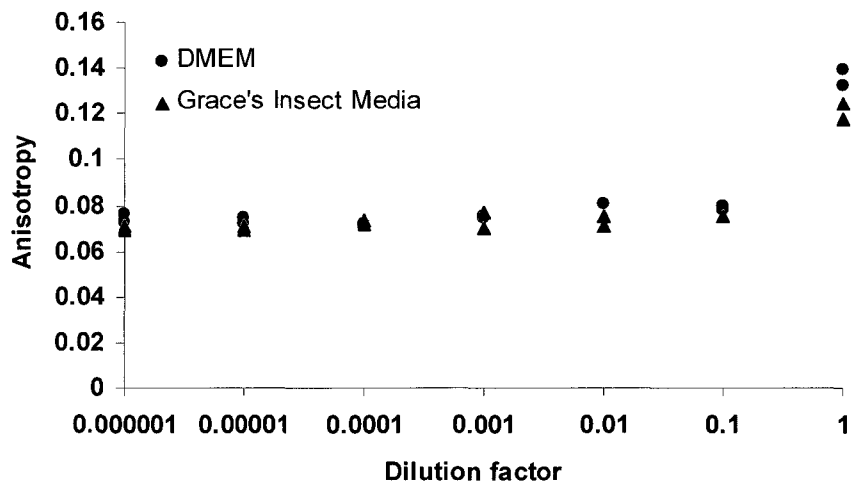

D

Figure 24: Fluoresence anisotropy plots of virus targets. Measurements (•) are fitted using the Hill function (solid line). Assessment of fit using R^2 value (inset) is displayed for viral targets. X-axis is plotted logarithmically for better visualization of K_D region. (A) MNV (B) GII.3 (C) FCV and Random sequence (D) Sera Controls (DMEM and Grace's Insect Media).

AG3 also demonstrated low affinity towards other targets. The estimated K_D for its interaction with FCV was around 5 x 10^{-8} M; six orders of magnitude weaker than its selected target. Furthermore, a random sequence (Figure A9, Appendix) of approximately the same length as AG3 appeared to show a similar behaviour to FCV (estimated K_D at 1 x 10^{-7} M), which provides supplemental support for specificity of AG3 towards norovirus targets. Again, it is not clear whether or not the binding reaches a saturation limit at the highest available concentration. However in the context of aptamer binding, any dissociation constant that lies above micromolar (10^{-6} M) concentration is considered to have weak affinity and would be impractical for biosensor applications.

It is emphasized that the K_D values for norovirus targets are estimates thus far. Evidently, the data points of the norovirus plots do not fully plateau since the experiments are limited by the highest concentration achieved for these targets. Virus yield from tissue culture can be unpredictable, since it is dependent on the efficiency of the viral expression, which can vary for different tissue culture systems. Higher target concentrations obtained would certainly allow for more data points collected and thus for completion of the binding curve. In addition, a second binding experiment that assesses the K_D in an alternative way would also be insightful in verifying the degree of aptamer affinity. For instance, a gel-shift assay [56] could be conducted on the monomer capsid at different concentrations and provide more visual measurements of aptamer affinity by observing at which protein concentration unbound DNA is minimally detected. Other examples include equilibrium dialysis and SPR [97, 66], which would measure rate constants that would allow the determination of the K_D for comparison.

4. Future studies

Further studies are suggested herein to provide additional insight into the binding mechanism of the aptamer candidates with norovirus as well as provide insight into the potential of the candidates as aptasensors. For instance, three-dimensional computational methods such as MC-Fold [98] would be useful to predict binding site specifics, given the sequences of the aptamer candidate and the protein monomer. This could also act as a premise for the experimental design of binding studies. Another consideration is that since clones AG28 and AG29 have yet to be investigated for binding, it would be interesting to assess their dissociation constants both separately from and collectively with AG3. This would determine a "best affinity scenario" for later aptasensing applications. Additionally, truncation studies may be considered to observe the effect on binding affinity and specificity (influence of primer sequences, minimal aptamer determination, etc.).

To take this experiment one step further, these studies could be conducted under more situational conditions. The discussed experiments were conducted in a buffer that mimicked the salinity and pH conditions of a meat sample. Realistically, however, a meat sample is a far more complex chemical matrix containing various non-specific components such as enzymes, salts, proteins and potentially other viruses. Conducting some of these studies in a spiked meat juice matrix, could help to further validate aptamer affinity and specificity and also provide preliminary observations that would contribute to optimizing an aptasensor platform. One proposed aptasensing platform is to create a

sandwich ELISA assay where a capture and reporter aptamer are incorporated rather than antibodies, on a microplate. The capture aptamers would bind with the virus particles and the reporter aptamers would follow suit but also behave as a secondary antibody by modifying one end with a fluorophore. This would generate a measureable signal that would determine a rapid positive test for the presence of norovirus, which could then be implemented in the field.

IV. Conclusions

Aptamer candidates have been selected for the detection of noroviruses using the process of SELEX. Nine rounds of selection against MNV resulted in three sequences as potential aptamer candidates. While the expression of GII.4 capsid particles was fruitless, an expression of GII.3 permitted for validation studies with selected aptamer candidates against its murine equivalent in hopes of having a ligand of similar affinity. Binding studies thus far demonstrate promise in affinity and selectivity of candidate sequence AG3, however, further insight into the full binding profile across larger scales of virus will allow for a more concrete determination of binding saturation and ultimately dissociation constants, via fluoresence anisotropy. With this confirmation for the aptamer candidates, an aptamer-based sensor may be established for detection of noroviruses in the meat production chain.

Acknowledgements

There are many people I wish to thank not only for the accomplishment of this project but also for the remarkable graduate school experience. First and foremost, I wish to thank Dr. Maria DeRosa for taking an interest in me all those years ago when I was only a 3rd year- undergraduate and for her ongoing support and encouragement throughout the duration of my degree. Thanks to the members of DeRosa lab, both past and present, for making the lab workplace an enjoyable experience and for extending their guidance, knowledge and support. Notably, thanks to Maureen McKeague, Ryan Walsh, and Erin McConnell for their assistance in various trainings for SELEX.

I also wish to thank Dr. Kirsten Mattison for giving me the opportunity to work in her laboratory as well as her guidance, encouragement and support. Thanks to past and present members of the virology lab, and to fellow employees of Health Canada's Bureau of Microbial Hazards for such a welcoming and friendly work environment. In particular, thanks to Anu Shukula-Jones for her training and assistance in my transition to the world of microbiology. Thanks to Oksana, Jen, Sara, Alex and Safaa for their donations of various lab samples and for their continuous support (not to mention also for getting me addicted to sushi!). Furthermore, I wish to thank Aaron Farnsworth and Michelle Lemieux for assistance with equipment.

Many thanks to our collaborators at CREM: Dr. Syed Sattar, Dr. Susan Springthorpe and Jason Tetro for their ongoing support, encouragement and guidance. It has been a pleasure to work with them. Thank you to the members of my defense committee for taking the time to read through this story about aptamers and viruses.

Last but certainly not least, thanks to my family-Mom, Dad, Gabe and Renato as well as my dearest friends- Tariq, Andrea and Mike, for their unconditional love and support throughout my degree. Finally, to all my friends both inside and outside of the Carleton Chemistry Department (too many to name here but you know who you are!), thank you all for your friendship and support. Best wishes to all of you in your future endeavours! ☺

VI. Appendix

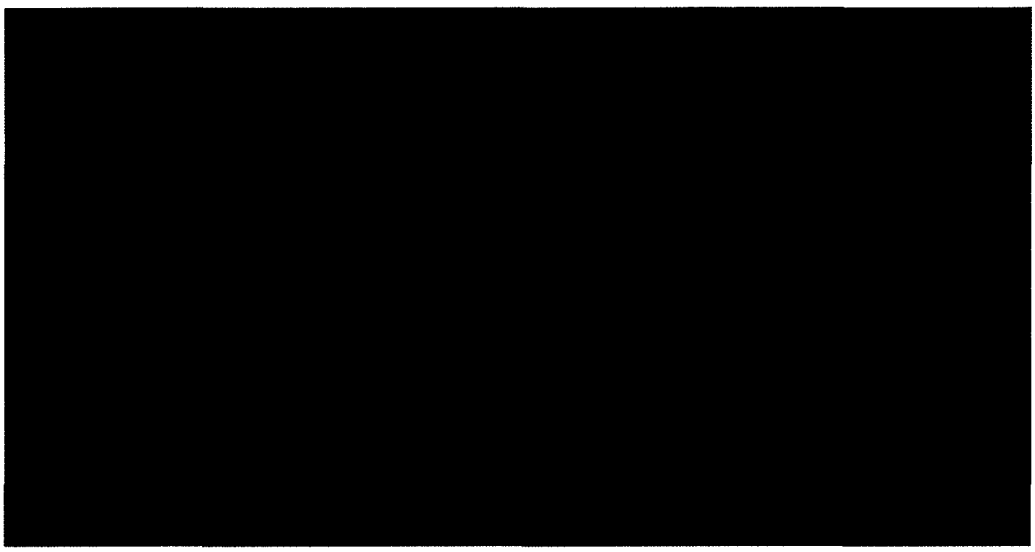

Figure A1: Agarose gel characterization of intact PVL+GII.4 plasmid. Samples are as follows (L to R): 1kb DNA LADDER, empty vector, 5 x pUC+GII.4, 5 x pVL+GII.4.

Figure A2: SDS-PAGE characterization of GII.4 Protein expression Experiment #1. Sample-containing lanes are as follows: 4-VL-1; 6-VL-3; 8-negative control, 10-AcNPV, 12-W2, 13-MB40, 14-809, 15-1kb LADDER.

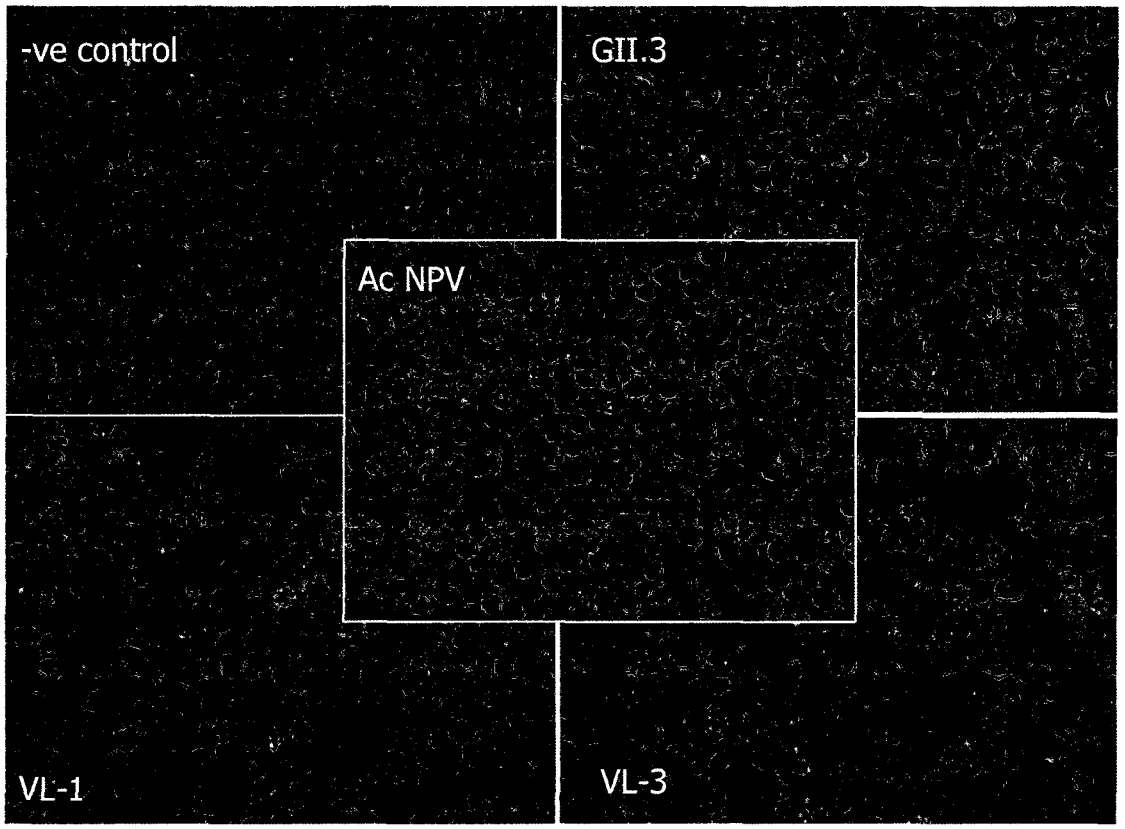

Figure A3: Observations from GII.4 protein expression experiment #3 (MOI~3, t= 4days)

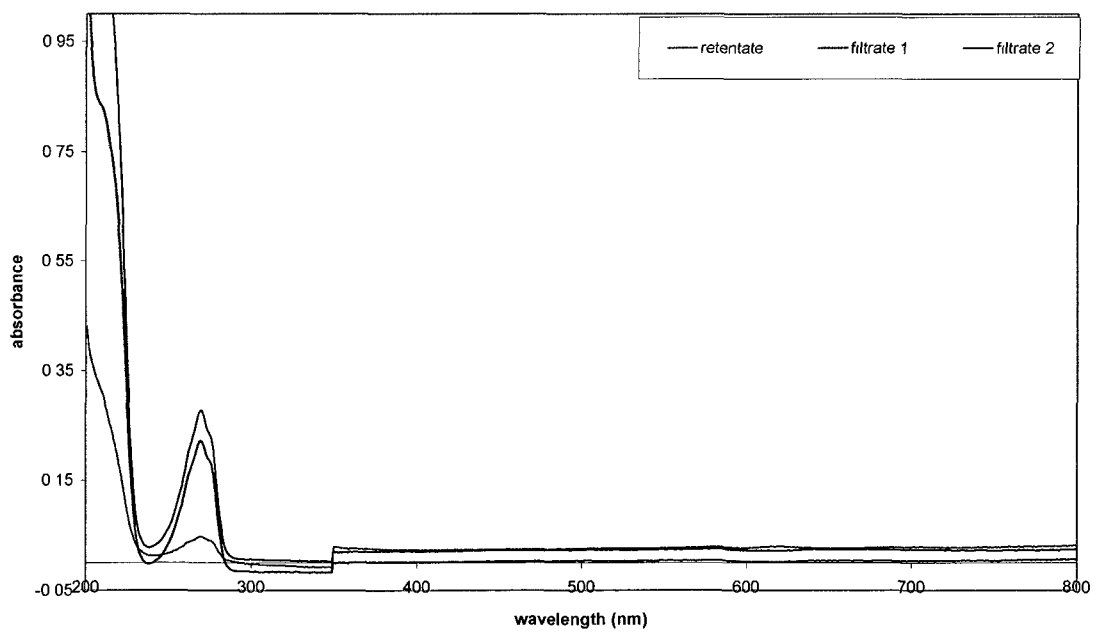

Figure A4: Round 3 observations of retained DNA cleanup prior to PCR amplification. Retentate

(pink) signal refers to the purified aptamer pool while filtrate signals 1 and 2 (green and red signals) refer to removed impurities.

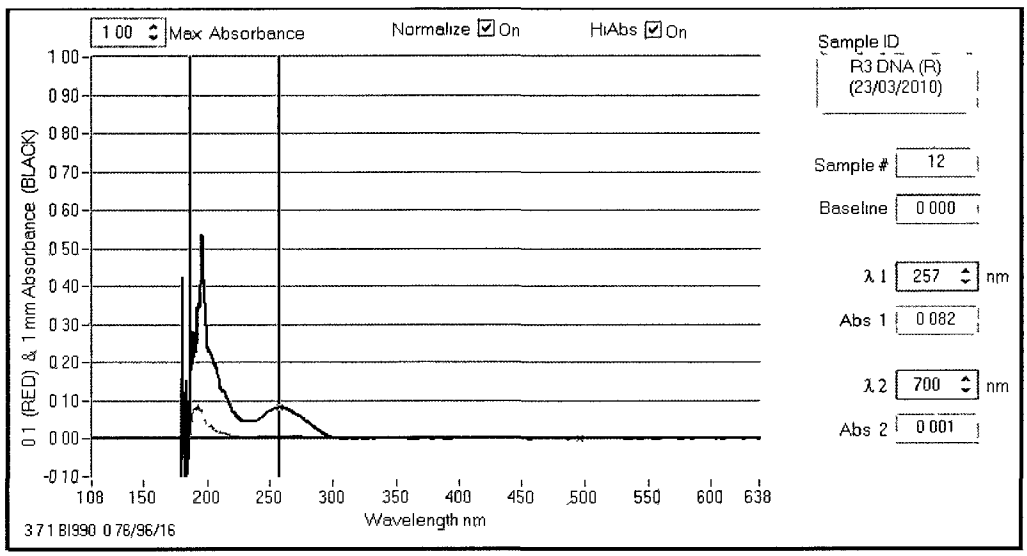

Figure A5: NanoDrop spectra of check for binding DNA in Round 3 for comparison.

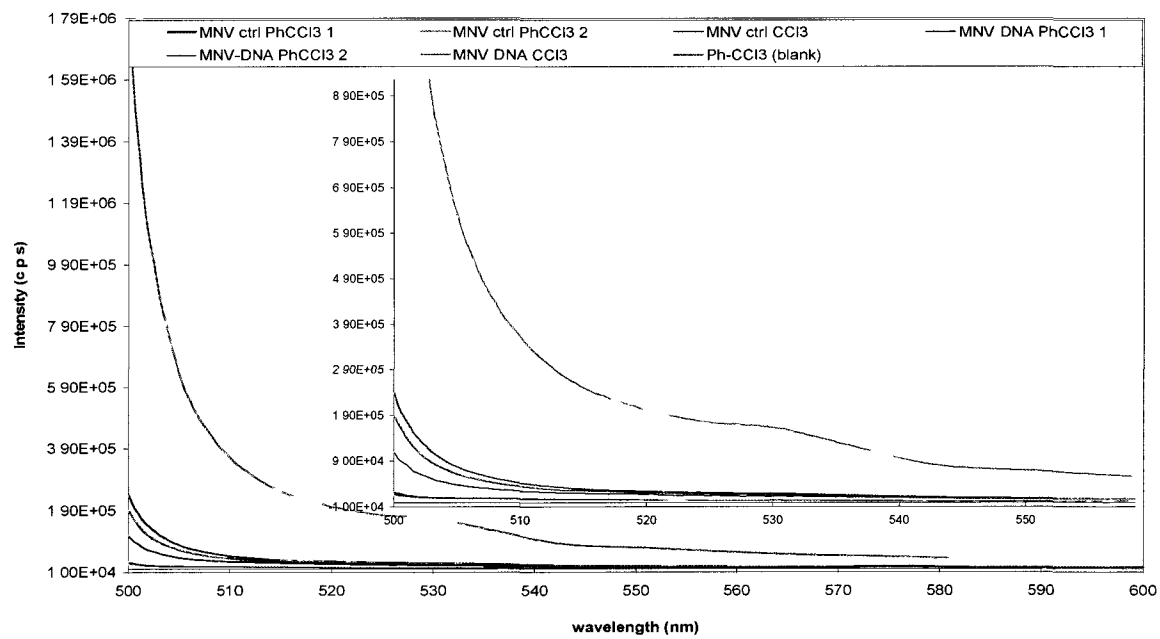

Figure A6: Emission spectra of components from phenol-chloroform extraction in Round 3 for fluorescein detection. Inset is a zoom-in of the signals measured for clarity.

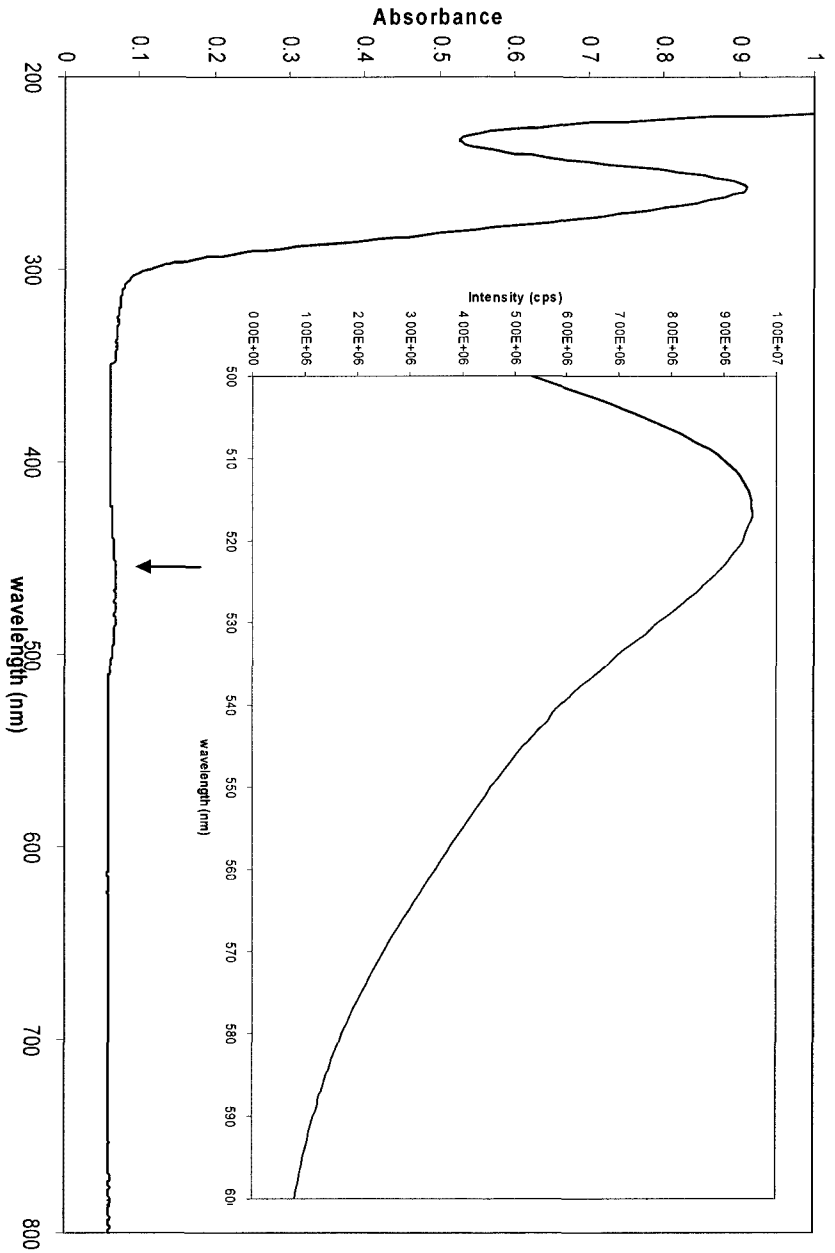

Figure A7: UV-Vis absorption and fluoresence emission spectra (inset) of fluorescein-tagged aptamer pool, post-round. Maxima are observed here at λ_{abs}=257nm for DNA and λ_{em}=518nm for fluorescein. A faint absorbance signal at approximately 490nm is additionally observed for fluorescein (arrow).

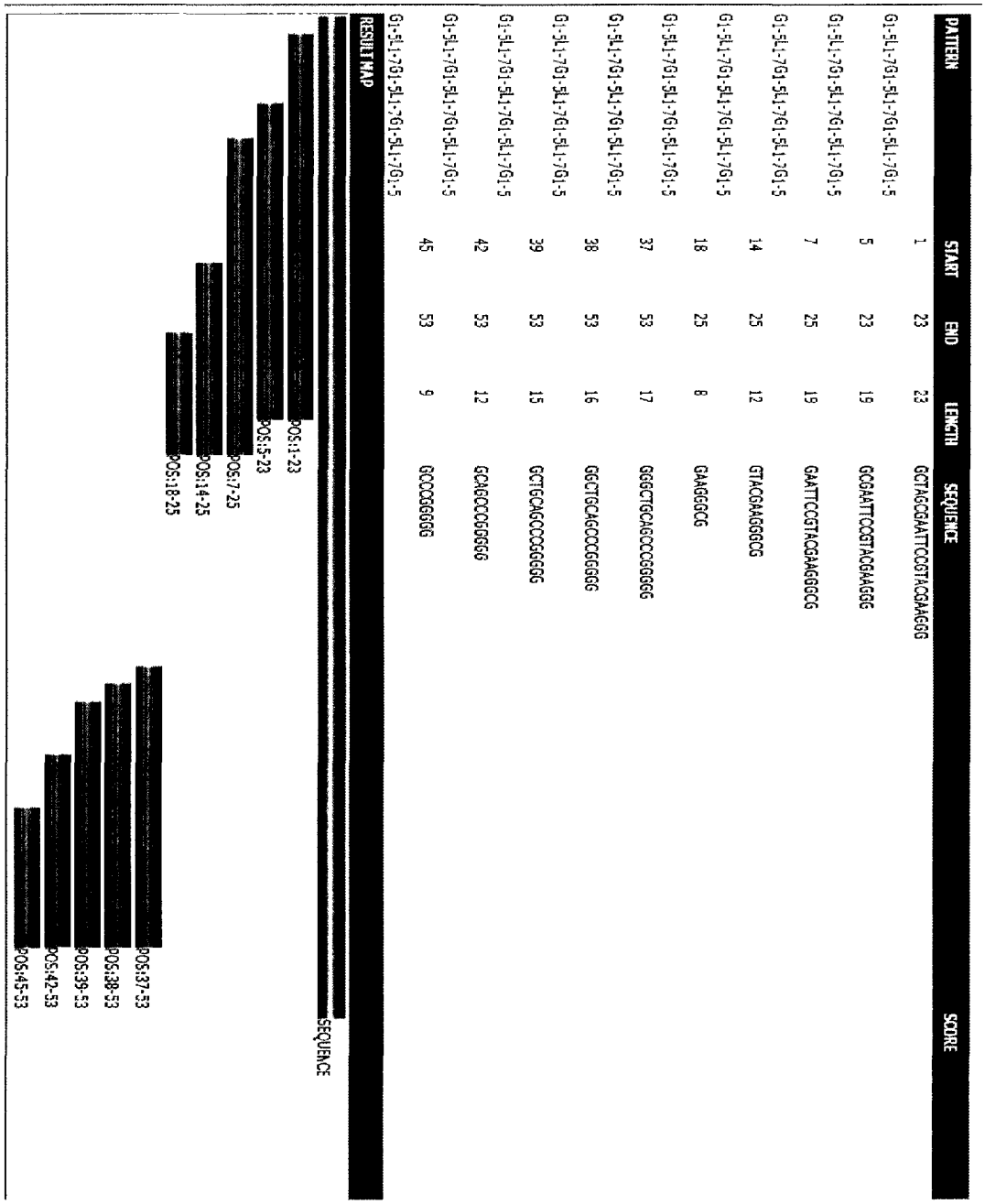

Figure A8: Snapshot of QuadFinder analysis for AG3 sequence. Online program lists potential areas of G-quadruplex formation on the input sequence and also illustrates the regions on a result map.

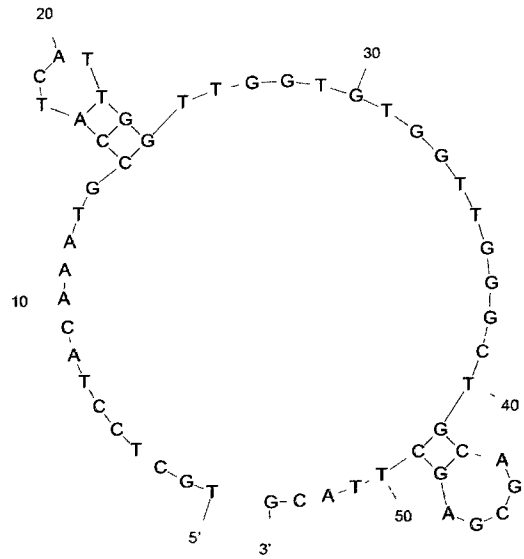

Figure A9: MFold prediction of the random sequence (54nt) used as a control.

VII. References

[1] "Foodborne Outbreak Investigations-The Food Production Chain". Centres for Disease Control and Prevention.
http://www.cdc.gov/outbreaknet/investigations/production_chain.html.
Accessed May 22, 2011.

[2] Government of Canada. "Report of the Independent Investigator into the 2008 Listeriosis Outbreak." Chapter 5. (July 2009).
http://www.listeriosis-listeriose.investigation-enquete.gc.ca/lirs_rpt_e.pdf
Accessed May 22, 2011.

[3] Balaban, N. and Rasooly, A. *International Journal of Food Microbiology.* 61 (2000) 1–10.

[4] Sugiyama, H. *Journal of Bacteriology.* 1951 July; 62(1): 81–96.

[5] "Hazard Analysis Critical Control Point System". World Health Organization.
http://www.who.int/foodsafety/fs_management/haccp/en/
Accessed May 22, 2011.

[6] Ministry of Health and Long-Term Care. Descriptive epidemiology of enteric outbreaks reported in Ontario, 2003.
www.health.gov.on.ca/ english/providers/pub/phero /pdf/2004/phero_1104.pdf
(Version current at May 16, 2006). Acccessed May 23, 2011.

[7] Mattner F, Sohr D, Heim A, Gastmeier P, Vennema H, Koopmans M. *Clin Microbiol Infect.* 2006 Jan; 12(1):69-74.

[8] CDC. "Updated Norovirus Outbreak Management and Disease Prevention Guidelines", 2011. *Morb. Mortal. Wkly Rep.* **60**, 1–15.

[9] Adler, J.L., Zickl, R. *J. Infect. Dis.* (1969) **119**, 668-73.

[10] Caul, O.E. *The Lancet* (1994) **343**(8908), 1240-1242.

[11] Mattison K, Shukla A, Cook A, Pollari F, Friendship R, Kelton D, Bidawid S, Farber JM. *Emerg Infect Dis.* (2007) **13**(8), 1184-8.

[12] van der Poel WH, *et al.*. *Vet Microbiol.*, (2003) **92**(4), 297-309

[13] Mattison K, Harlow J, Morton V, Cook A, Pollari F, Bidawid S, et al. *Emerg. Infect. Dis.*, (2010) **16**(11), 1815-1817.

[14] Nilsson, M. *et al. J.Virol.* (2003) **77**, 13117-13124.

[15] Hutson, A.M., Atmar, R.L., Graham, D.Y., and M.K Estes. *J. Infect. Dis.* (2002) **185**, 1335-1337.

[16] Flint. *et. al.* (2005) *Emerg. Infect. Dis.* **41**, 698-704.

[17] Donaldson, E.F. *et al.* (2010) *Nat. Rev. Microbiol.* **8**, 231-241.

[18] Tan *et al.* "Molecular Pathogenesis of Human Noroviruses". RNA Viruses, Chapter 24, p. 575-600.

[19] Scipioni *et al.* (2008) *The Veterinary Journal.* **178,** 32-45.

[20] Wobus, CE , Thackray, LB and Virgin IV, HW, *J. Virol.* (2006) **80** (11), 5104-5112.

[21] Murphy, C.I. and Piwnica-Worms, H. "Overview of the Bacculovirus Expression Vector System". *Current Protocols in Neuroscience* (2000) Unit 4.18, Supplement 10. pp 1-4.

[22] PharMingen. "Bacculovirus Expression Vector System Manual". 6th Edition, 1999.

[21] Duizer, E., K. J. Schwab, F. H. Neill, R. L. Atmar, M. P. Koopmans, and M. K. Estes. 2004. *J. Gen. Virol.* **85:**79–87.

[22] Tan M, Xia M, Chen Y, Bu W, Hegde RS, *et al. PLoS ONE* (2009) **4**(4), e5058 1-10.

[23] Hardy, M.E. *FEMS Microbiol.* Lett. (2005) **253**, 1–8.

[24] Rohayem, J., *et al. J.Gen. Virol.* (2006) **87**, 2621-2630.

[25] "Bioterrorism agents/diseases" (2009). http://www.bt.cdc.gov/agent/agentlist-category.asp . Accessed June 1, 2011.

[26] Katpally, U. *et al. J.Virol.* (2008), **82**(5), 2079-2088.

[27] Furman *et al. Virology Journal* (2009) **6**(139), 1-11.

[28] Wobus CE, *et al.*. *Plos Biology* (2004) **2,** 2076-2084.

[29] Atmar and Estes (2001) *Clin. Microbiol. Rev.* **14**, 15–37.

[30] Beuret, C.M. *Methods in Biotechnology* Vol. 21: *Food-borne Pathogens: Methods and Protocols.* Chapter 24. p.135-152.

[31] Burton-MacLeod *et al.* (2004) *J. Clin. Microbiol.* **42**, 2587–2595.

[32] deBruin *et al.* (2006) *Journal of Virological Methods* **137**, 259–264.

[33] Richards *et al.* (2003) *J. Clin. Microbiol.* **26**, 109–115.

[34] Mattison, K. *et al.* (2011) *Journal of Clinical Virology* **50** *109–113.*

[35] Bessetti, J., Promega Corporation *Profiles in DNA* (2007), **10**(1), 9–10.

[36] Krause *et al. Applied and Environmental Microbiology*, Aug. 2006, **72**(8), 5463–5468.

[37] Q-H Wang *et al.* (2006) *J. Virol Meth.* **132** 135–145.

[38] Martella *et al.* (2007) *Emerg Infect. Dis.* **13**(7), 1071-1073.

[39] Mesquita *et al.* (2010) *Emerg Infect Dis.* **16**(6), 980–982.

[40] Ricci, F. *et al.* (2007) *Analytica Chimica Acta* **605**(2), 111-129.

[41] Ellington, A. D. & Szostak, J. W. *Nature* **346**, 818–822 (1990).

[42] Tuerk, C. & Gold, L. *Science* **249**, 505–510 (1990).

[43] J Lee *et al.* Nucleic Acids Research, 2004, Vol. 32, Database issue D95-D100.

[44] Stojanovic, M. and Landry, D. *J. Am. Chem. Soc.* **2002**, 124, 9678-9679.

[45] Xiao, Z. *et al.* (2008) *Chem. Eur. J.* **14**, 1769 – 1775

[46] Luo, X.; McKeague M., *et al.* (2010) *RNA* **16** (11), p 2252-2262.

[47] McKeague, M., *et al.* (2010) *Int. J. Mol. Sci* **11**, 4864-4881.

[48] Stoltenburg R., Reinemann C., and Strehlitz B. *Biomolecular Engineering* (2007) **24**, 381–403

[49] Cruz-Toledo J, McKeague M, Zhang X, Giamberardino A, McConnell E, Francis T, DeRosa M.C and Dumontier M. *Database : The Journal of Biological Databases and Curation.* Manuscript in preparation for 2011 special issue.

[50] Bartel, D. P., & Szostak, J. W. *Science.*(1993) **261**, 1411-1418.

[51] Hirao I. *et al.* (1999) *Molecular Diversity* **4**, 75-89.

[52] James, W. "Aptamers" Encyclopedia of Analytical Chemistry R.A. Meyers (Ed.) pp. 4848–4871. John Wiley & Sons Ltd, Chichester, 2000.

[53] Klussmann, S. and Eulberg, D. *Chem Bio Chem.* (2003) **4**, 979-983.

[54] DJ Patel, *et al.* (1997), *J. Mol. Biol.*, **272**(5), 645–664.

[55] Ogasawara *et al.* (2007) *Prion,* **1**(4), 248-254.

[56] Mascini, Marco. Aptamers in Bioanalysis. Wiley & Sons. New Jersey, 2009.

[57] Berezovski, M. and Krylov, S.N. *Anal. Chem.* (2005), **77**, 1526-1529.

[58] Gopinath, SCB *et al.* (2007) *Anal Bioanal Chem.*, 3**87**, 171–182.

[59] Cox JC, Rudolph P and Ellington AD. (2008) *Biotechnol. Prog.* **14**(6), 845-850.

[60] Williams, K.P., Bartel, D.P., *Nucleic Acids Res.* (1995) **23**, 4220–4221.

[61] Bock, L.C *et al.* (1992) *Nature* **355**, 564-566.

[62] Dang C. and Jayasena, S.D. *J. Mol. Biol.* (1996) **264**, 268–278.

[63] "Recombinant DNA and Gene Cloning." http://users.rcn.com/jkimball.ma.ultranet/BiologyPages/R/RecombinantDNA.html. Updated March 12, 2011, Page Accessed July 21, 2011.

[64] Jing M. and Bowser, M.T. *Analytica Chimica Acta* (2011) **686,** 9–18.

[65] Mairal T. *et al.* (2008) *Anal. Bioanal. Chem.* **390**, 989–1007.

[66] Keefe A.D., Pai S., and Ellington A.D. *Nature Reviews* (2010) **9,** 537-550.

[67] Zelada-Guillen, *et al.* (2010). *Anal. Chem.,* **82** (22), 9254-9260.

[68] Bruno *et al.* (2009) *Journal of Fluorescence,* **19**(3), (427-435).

[69] McKeague M, Giamberardino A, and DeRosa, M.C. (2011) "Advances in Aptamer-Based Biosensors for Food Safety". In Vernon Somerset (Ed.), *Biosensors for Health, Environment and Biosecurity.* (pp.17-42). InTech, Available from: http://www.intechopen.com/articles/show/title/advances-in-aptamer-based-biosensors-for-food-safety.

[70] Lee J.F, Stovall G.M and Ellington, A.D. *Curr Opin Chem Biol.* (2006) **10**, 282–289

[71] Jang K.J, *et al.* (2008) *Biochem Biophys Res Comm.* **366** (3), 738-744.

[72] Harris, D.C, Quantitative Chemical Analysis. 6th ed. W.H Freeman and Company. New York, 2003. pp 439.

[73] Goutelle, S. *et al.* (2008) *Fundamental & Clinical Pharmacology* **22**, 633–648.

[74] Rippe, K. *B.I.F. Futura* (1997) **12**, 20-26.

[75] Perrin, W.F. *J. Phys. Radium V.* (1926) **7** 390-401.

[76] Polarization Technical Resource Guide. 4th ed. Chapter 7: "Theory of Binding Data Analysis Fluorescence". Invitrogen, 2006. https://tools.invitrogen.com/content.cfm?pageid=9880&CMP=ILC-FPGUIDE Accessed July 21, 2011.

[77] Di Martino, B and Marsilio, F. *Research in Veterinary Science* (2010) **89**, 279-281.

[78] Sambrook et al., Molecular Cloning, a Laboratory Manual, 2nd Ed., vol.2, Chpt. 9, "Analysis and Cloning of Eukaryotic Genomic DNA"; Chpt. 10, "Preparation of Radiolabled DNA and RNA Probes"; and Chpt. 11, "Synthetic Oligonucleotide Probes". pp. 24-28.

[79] Protein Calculator v.3.3. http://www.scripps.edu/~cdputnam/protcalc.html. Updated March 2006.

[80] Hartmann, Roland K. Handbook of RNA biochemistry Vol. 2. (pp.823-824).

[81] Sambrook, J., E.F. Fritsch and T. Maniatis (2001) "Recovery of Synthetic Oligonucleotides by Electrophoresis Through a Denaturing Polyacrylamide Gel". *Molecular Cloning, a laboratory manual.* 3rd ed. Cold Spring Harbor Laboratory, Cold Spring Harbor, NY. pp 11.23-11.28

[82] Niazi, J.H. *et al.* (2008) *Bioorganic & Medicinal Chemistry* **16**, 1254–1261.

[83] Liu, Li-Juan *et al.* (2010) *Am. J. Trop. Med. Hyg.*, **82**(4), 717–722.

[84] van Oers, M.M (2011) *Journal of Invertebrate Pathology* **107**, S3-S15.

[85] Applied Biosystems "The Basics: Northern Analyis". http://www.ambion.com/techlib/basics/northerns/ Updated 2011.

[86] BD Biosciences. "Baculovirus Protein Expression-Plaque Assay". http://www.bdbiosciences.com/support/resources/baculovirus/plaque_assay.jsp. Updated 2011, Accessed August 16, 2011.

[87] Lindesmith, L.C *et al.* (2008) *PLoS Medicine* **5**(2), 0269-0290.

[88] Hardy et *al.* (1995) *J.Virol.* **69**(3), 1693-1698.

[89] Luttermann, C and Meyers, G. (1995). "Feline Calicivirus". Hansman,G.S, Jiang, X,J and Green, K.Y.(Eds.), *Caliciviruses: Molecular and Celular Virology.*(pp146-168). Caister Academic Press, Norfolk UK.

[90] "Technical Resources - Media Formulations 12400 - D-MEM/F-12, powder, HEPES". Invitrogen. http://www.invitrogen.com/site/us/en/home/support/Product-Technical-Resources/media_formulation.59.html Updated 2011.

[91] Allen, D.J *et al.* (2009) *Virology Journal* , **6**(150), 1-11.

[92] "Nucleic Acid Extraction". Uptima. http://www.interchim.com/interchim/bio/produits_uptima/product_line/nucleicacid_extraction.htm. Page Accessed August 16, 2011.

[93] Lindquist, L. *Arkiv.Kemi.* (1960) **16** 79-138. http://www.exiqon.com/ls/homeofIna/Chemistry/Fluorescein.pdf

[94] Cavaluzzi M.J and Borer P.N. *Nucleic Acids Res.* 2004, **32**(1), e13, 1-9.

[95] QuadFinder Version 1.0. Institute of Genomics and Integrative Biology. http://miracle.igib.res.in/cgi-bin/quadfind/gquad.pl. Accessed August 16, 2011.

[96] White *et al.* (2001) *Molecular Therapy* **4**(6), 567-573.

[97] Braunlin WH, Strick, TJ and Record Jr., MT (1982) *Biopolymers* **21**(7), 1301-1314.

[98] "MC-Fold". http://www.major.iric.ca/MC-Fold/. Accessed August 27, 2011.